Chronic overexpression of PNPLA3^{I148M} in mouse liver causes hepatic steatosis

John Zhong Li,[1] Yongcheng Huang,[1] Ruchan Karaman,[1] Pavlina T. Ivanova,[2] H. Alex Brown,[2] Thomas Roddy,[3] Jose Castro-Perez,[3] Jonathan C. Cohen,[1] and Helen H. Hobbs[1,4]

[1]Departments of Molecular Genetics and Internal Medicine, Eugene McDermott Center for Human Growth and Development, University of Texas Southwestern Medical Center, Dallas, Texas, USA. [2]Departments of Pharmacology and Chemistry, Vanderbilt University, Nashville, Tennessee, USA. [3]Atherosclerosis Merck Research Laboratories, Rahway, New Jersey, USA. [4]Howard Hughes Medical Institute, University of Texas Southwestern Medical Center, Dallas, Texas, USA.

A genetic variant in *PNPLA3* (*PNPLA3^{I148M}*), a triacylglycerol (TAG) hydrolase, is a major risk factor for nonalcoholic fatty liver disease (NAFLD); however, the mechanism underlying this association is not known. To develop an animal model of PNPLA3-induced fatty liver disease, we generated transgenic mice that overexpress similar amounts of wild-type PNPLA3 (PNPLA3^{WT}) or mutant PNPLA3 (PNPLA3^{I148M}) either in liver or adipose tissue. Overexpression of the transgenes in adipose tissue did not affect liver fat content. Expression of PNPLA3^{I148M}, but not PNPLA3^{WT}, in liver recapitulated the fatty liver phenotype as well as other metabolic features associated with this allele in humans. Metabolic studies provided evidence for 3 distinct alterations in hepatic TAG metabolism in PNPLA3^{I148M} transgenic mice: increased formation of fatty acids and TAG, impaired hydrolysis of TAG, and relative depletion of TAG long-chain polyunsaturated fatty acids. These findings suggest that PNPLA3 plays a role in remodeling TAG in lipid droplets, as they accumulate in response to food intake, and that the increase in hepatic TAG levels associated with the I148M substitution results from multiple changes in hepatic TAG metabolism. The development of an animal model that recapitulates the metabolic phenotype of the allele in humans provides a new platform in which to elucidate the role of PNLPA3^{I148M} in NAFLD.

Introduction

Higher organisms stockpile triacylglycerol (TAG) in adipose tissue as a buffer against fluctuations in food availability and energy demands. TAG is usually maintained at much lower concentrations in other tissues. In several species, including migratory birds, mice, and humans, sustained caloric excess causes TAG to accumulate in nonadipose tissues, particularly liver (1, 2). In humans, the propensity to accumulate hepatic TAG varies widely among individuals: hepatic TAG content ranges from <1% to >50% of liver weight (3). Several factors are associated with an increase in liver TAG content, including obesity, insulin resistance, and alcohol ingestion, but the factors responsible for the wide interindividual differences in hepatic TAG levels have not been fully elucidated (4, 5).

In 2008, we identified a missense sequence variation (I148M) in patatin-like phospholipase domain-containing 3 (PNPLA3, alternatively referred to as adiponutrin) (6) that is associated with increased hepatic TAG content (7). Homozygotes for the variant allele (148M) have a 2-fold higher hepatic TAG content than do homozygotes for the wild-type allele (148I). The 148M variant has been shown to be associated with the full spectrum of nonalcoholic fatty liver disease (NAFLD): hepatic steatosis, steatohepatitis, cirrhosis, and hepatocellular carcinoma (8–17). Moreover, among alcoholics, the risk of developing cirrhosis is increased 3.5- to 4-fold in homozygotes for the 148M variant (14, 18, 19). These findings are consistent with PNPLA3 playing a role in metabolism of hepatic TAG, but the normal physiologic role of the enzyme and how the 148M isoform causes liver disease remain obscure.

PNPLA3 belongs to a family of proteins that share a domain that was first identified in patatin, a major soluble protein of potato tubers with nonspecific acyl hydrolase activity (20). The domain differs from classical lipases by employing a catalytic dyad (Ser-Asp), rather than a catalytic triad, to effect hydrolysis (21). PNPLA3 is expressed primarily in liver and adipose tissue, in which it partitions to membranes and lipid droplets (22). Biochemical studies using purified recombinant human PNPLA3 indicate that the enzyme hydrolyzes acylglycerols (monoacylglycerols, diacylglycerols [DAGs], and TAGs) with first-order Michaelis-Menten kinetics but has little to no activity against phospholipids (23). The I148M substitution markedly reduces acylglycerol hydrolase activity, decreasing the V_{max} of the enzyme, without reducing substrate affinity. These findings are consistent with a structural model of the patatin domain of PNPLA3, in which the substitution of methionine for isoleucine at residue 148 blocks access of substrate to the catalytic serine (22). Thus, the in vitro data suggest that the enzyme normally functions as an acylglycerol hydrolase and that the I148M substitution causes a loss of hydrolytic function, resulting in accumulation of excess TAG.

Data from genetically manipulated mice are difficult to reconcile with a loss-of-function model. Inactivation of *Pnpla3* in mice does not result in any change in hepatic TAG content (24, 25), even when the mice are challenged with a high-sucrose diet. In addition, overexpression of wild-type PNPLA3 by adenoviral transgenesis does not reduce liver TAG levels (22). Conversely, adenovirus-mediated overexpression of PNPLA3^{I148M} in mouse liver causes an increase in hepatic TAG content, which is more consistent with the I148M substitution conferring a gain of function (22). Recently, Kumari et al. (26) reported that PNPLA3 had lysophosphatidic acid acyltransferase (LPAAT) activity and that the I148M substitution increases

Conflict of interest: Thomas Roddy and Jose Castro-Perez work for Merck. Merck provided no financial support for the experiments.

Citation for this article: *J Clin Invest.* 2012;122(11):4130–4144. doi:10.1172/JCI65179.

rather than decreases this activity, suggesting that the I148M variant may cause hepatic steatosis by increasing TAG synthesis.

The regulation of PNPLA3 also suggests that the enzyme plays a role in lipid anabolism, rather than catabolism. The protein is highly regulated by nutritional stimuli at both the transcriptional and posttranslational levels (27, 28). Regulation is coordinated by the transcription factors liver X receptor (LXR) and SREBP-1c (28). During fasting, low levels of SREBP-1c result in low transcription of *PNPLA3* mRNA and efficient degradation of PNPLA3 protein, ensuring very low levels of PNPLA3 in the liver. With carbohydrate refeeding, insulin upregulates SREBP-1c, which in turn stimulates PNPLA3 transcription and concomitantly upregulates fatty acid biosynthesis. Endogenously synthesized fatty acids retard the degradation of PNPLA3 protein, leading to a marked postprandial rebound in PNPLA3 levels (28). Thus, *PNPLA3* is upregulated when the liver is synthesizing TAG and sequestering it in lipid droplets.

To elucidate the mechanism by which the PNPLA3^{I148M} variant confers susceptibility to fatty liver disease, we sought to develop an animal model that recapitulates the human phenotype associated with this allele. Since deletion of *Pnpla3* in mice does not lead to increased liver fat content (24, 25), we developed transgenic mice that overexpress either wild-type or mutant (148M) human PNPLA3 in liver or in adipose tissue. Experiments were designed to address three fundamental questions. First, does the increased hepatic fat associated with the 148M variant result from the action(s) of the mutant allele in liver or in fat? Second, does the 148M variant promote the accretion or retard the degradation of hepatic TAG? Third, PNPLA3 has acyltransferase activity (29), and it has been speculated that the enzyme plays a role in TAG remodeling. Does expression of the 148M variant alter the spectrum of TAG species in the liver? Here, we show that overexpression of wild-type PNPLA3 in liver or in adipose tissue did not alter the total TAG content of either tissue, whereas overexpression of mutant PNPLA3 in liver, but not in adipose tissue, altered the level and composition of hepatic TAGs.

Results

Development of transgenic mice expressing human PNPLA3 (PNPLA3^{WT} and PNPLA3^{I148M}) in liver and adipose tissue. Lines of PNPLA3 transgenic mice in a C57BL/6J background were established that express wild-type human PNPLA3 (PNPLA3^{WT}) or the 148M variant (PNPLA3^{I148M}) in liver or in adipose tissue (L-PNPLA3^{WT} and L-PNPLA3^{I148M} or A-PNPLA3^{WT} and A-PNPLA3^{I148M}). Liver-specific expression was obtained by placing the transgenes under control of a liver-specific enhancer/promoter of ApoE (30). Two liver-specific lines expressing similar levels of hepatic wild-type and mutant mRNA and protein (PNPLA3^{WT} and PNPLA3^{I148M}, respectively) were selected for study (Figure 1A). Expression of both transgenes was largely confined to the liver. Low levels of *PNPLA3* mRNA were detected in the lungs of the PNPLA3^{WT} transgenic mice and in the brain, heart, kidney, lung, and spleen of the PNPLA3^{I148M} transgenic mice. Within the liver, more than 95% of the PNPLA3 protein was located in lipid droplets in both lines of mice (Supplemental Figure 1; for uncut gels see Supplemental Material; supplemental material available online with this article; doi:10.1172/JCI65179DS1), and within the lipid droplet fractions from the 2 lines the levels of PNPLA3 were similar (Figure 1A). The antibody used in this experiment recognizes human PNPLA3 and not mouse PNPLA3. Perilipin 2 (PLIN2), a lipid droplet protein, was used as a loading control. Transgenic mouse lines expressing wild-type and mutant human PNPLA3 in adipose tissue were generated by expressing the human PNPLA3 cDNAs under control of the aP2 promoter (ref. 31 and Figure 1B). As expected, the major site of expression of both transgenes was in adipose tissue. Expression levels of PNPLA3 were 3-fold higher in brown fat than in white fat (Figure 1B), which is similar to the expression pattern seen with this promoter in other transgenic lines (32, 33). Similar levels of PNPLA3 were present in the lipid droplets in the adipose tissues of the 2 transgenic mouse lines (Figure 1B).

Expression of PNPLA3^{I148M} in liver, but not adipose tissue, causes increased liver TAG. To assess the effect of hepatic PNPLA3 expression on the amount and distribution of neutral lipid in the liver, sections from the livers of 12-week-old chow-fed male mice were subjected to Oil Red O staining (Figure 2A). Lipid droplets in the livers of PNPLA3^{WT} transgenic mice were similar in size and distribution to those of wild-type animals, whereas mice expressing the 148M variant had an increase in both the number ($0.42 \pm 0.05/\mu m^2$ vs. $0.20 \pm 0.03/\mu m^2$) and the size ($0.098\ \mu m^2$ vs. $0.055\ \mu m^2$) of lipid droplets when compared with those of the wild-type transgenic mice. The increased neutral lipid content of livers from PNPLA3^{I148M} transgenic mice was confirmed biochemically (Figure 2A): TAG and cholesteryl esters were both increased 1.8-fold in the PNPLA3^{I148M} transgenic mice when compared with those in the PNPLA3^{WT} transgenic mice, but the absolute increase in the mass of TAG was much greater than that of cholesteryl esters (10 mg/g vs. 0.15 mg/g). Similar results were obtained using an independent line of PNPLA3^{I148M} transgenic mice (data not shown). Hepatic TAG levels tended to be lower in PNPLA3^{WT} transgenic mice than in their nontransgenic littermate controls, but the differences did not reach statistical significance in 3 independent experiments. No significant differences in hepatic levels of free cholesterol or phosphatidylcholine were apparent among the 3 lines of mice. Plasma levels of lipids and liver enzymes (aspartate transaminase [AST] and alanine transaminase [ALT]) did not differ among the 3 lines of chow-fed mice (Supplemental Figure 2A). Increased hepatic TAG content is often accompanied by insulin resistance, but no differences in plasma glucose levels were detected after fasting or in response to glucose or insulin challenges (Supplemental Figure 2B). Nor were any inter-line differences found in the relative amounts of phosphorylated AKT (Supplemental Figure 2C) in the liver. Serum levels of insulin also did not differ between the lines (Supplemental Figure 2D). Thus, the metabolic sequelae of overexpressing PNPLA3^{I148M} in livers of mice mirror the phenotype associated with the variant in humans (i.e., increased liver TAG content, without changes in plasma lipids or insulin sensitivity) (7).

Overexpression of PNPLA3^{I148M} in adipose tissue did not affect the lipid content of the liver (Figure 2B). Expression of wild-type or mutant PNPLA3 in adipose tissue was not associated with changes in fat cell morphology (Figure 2B), body weight, or distribution of body fat (Supplemental Figure 3A) or in plasma levels of lipids, glucose, or fatty acids (Supplemental Figure 3B). No significant changes in levels of expression of genes that regulate TAG metabolism were seen in either brown or white adipose tissue (BAT or WAT) (Supplemental Figure 3C). Recently, it was reported that *PNPLA3* mRNA levels are reduced in adipose tissue of rats exposed to the cold (34). To test whether overexpression of PNPLA3 in adipose tissue affects temperature control or response to cold exposure, body temperature was monitored in mice maintained at a temperature of 4°C for up to 3 hours. The reductions in body temperature of the transgenic lines were similar to those seen in the wild-type mice (Supplemental Figure 3D). Thus, we did not observe any effect

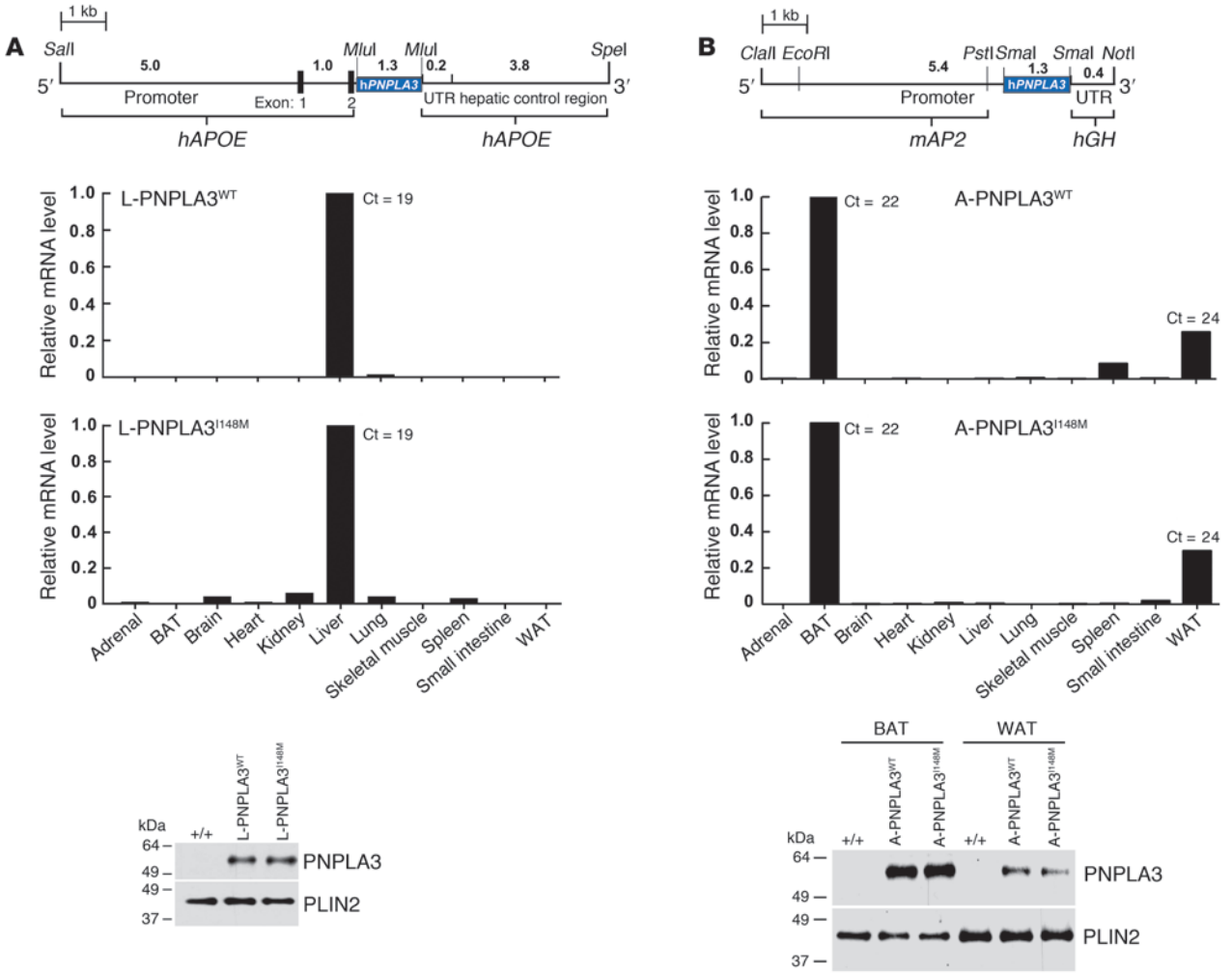

Figure 1

Tissue distribution of *PNPLA3* mRNA in transgenic mice expressing human PNPLA3 predominantly (**A**) in the liver or (**B**) in adipose tissue. (**A**) Schematic diagram of the PNPLA3 transgene, which is under control of a liver-specific enhancer/promoter element (30). Total mRNA was isolated from tissues of C57BL/6J mice expressing wild-type (L-PNPLA3^{WT}) or mutant (L-PNPLA3^{I148M}) human PNPLA3 (n = 4/group). Tissue levels of *PNPLA3* mRNA were determined using real-time PCR, as described in the Methods. The cycle threshold (Ct) value in the liver is provided. Each value in the nonhepatic tissues represents the mRNA level relative to the value in liver. Immunoblot analysis was performed on lipid droplets isolated from the livers (22). A total of 1% of the volume of each fraction was size fractionated on an 8% SDS-PAGE gel and probed using a polyclonal anti-human PNPLA3 antibody (22). PLIN2, a lipid droplet protein, was used as a loading control. (**B**) Schematic diagram of the constructs used to make the A-PNPLA3^{WT} and A-PNPLA3^{I148M} mice (31). Tissue levels of *PNPLA3* mRNA were measured by real-time PCR and expressed relative to the level in BAT. Immunoblot analysis of PNPLA3 in lipid droplets isolated from BAT and WAT was performed as described in **A**. UTR, untranslated region; *hAPOE*, human *APOE*; *mAP2*, mouse AP2; *hGH*, human GH.

of overexpressing PNPLA3 in adipose tissue on TAG or fatty acid metabolism in liver or adipose tissue. Accordingly, subsequent studies were performed only in the 2 lines of liver-specific transgenic mice, which are referred to as PNPLA3^{WT} and PNPLA3^{I148M}, and their nontransgenic littermates.

Dietary composition affects accumulation of hepatic TAG in PNPLA3^{I148M} mice. Hepatic TAG levels are strongly influenced by dietary carbohydrate and fat content. To determine the effect of dietary composition on the accumulation of hepatic fat in the wild-type and mutant transgenic mice, mice were fed a high-sucrose diet (58% sucrose, 0% fat) for 6 weeks. Hepatic TAG levels increased 3-fold in the PNPLA3^{I148M} transgenic mice when compared with PNPLA3^{WT} transgenic mice or nontransgenic controls (Figure 3A). An increase of similar magnitude was seen in cholesteryl ester levels in these mice. Mice were also challenged with a high-fat diet (45% animal fat). Hepatic TAG levels were increased to high levels in all the mice, but no differences were found between the lines, even when the diet was continued for 12 weeks (Figure 3B). The divergent responses to the 2 diets were not attributable to differences between the lines in body weight accrual or in body composition (Supplemental Figure 4). Plasma levels of lipids, fasting glucose, ketone bodies, nonesterified fatty acids (NEFAs), and liver enzymes did not differ between the lines on the different diets (Supplemental Figure 5).

Effect of PNPLA3^{I148M} on hepatic TAG metabolism. Liver TAG accumulation may be caused by increased TAG accrual or decreased TAG removal. To determine the effect of PNPLA3 expression on hepatic

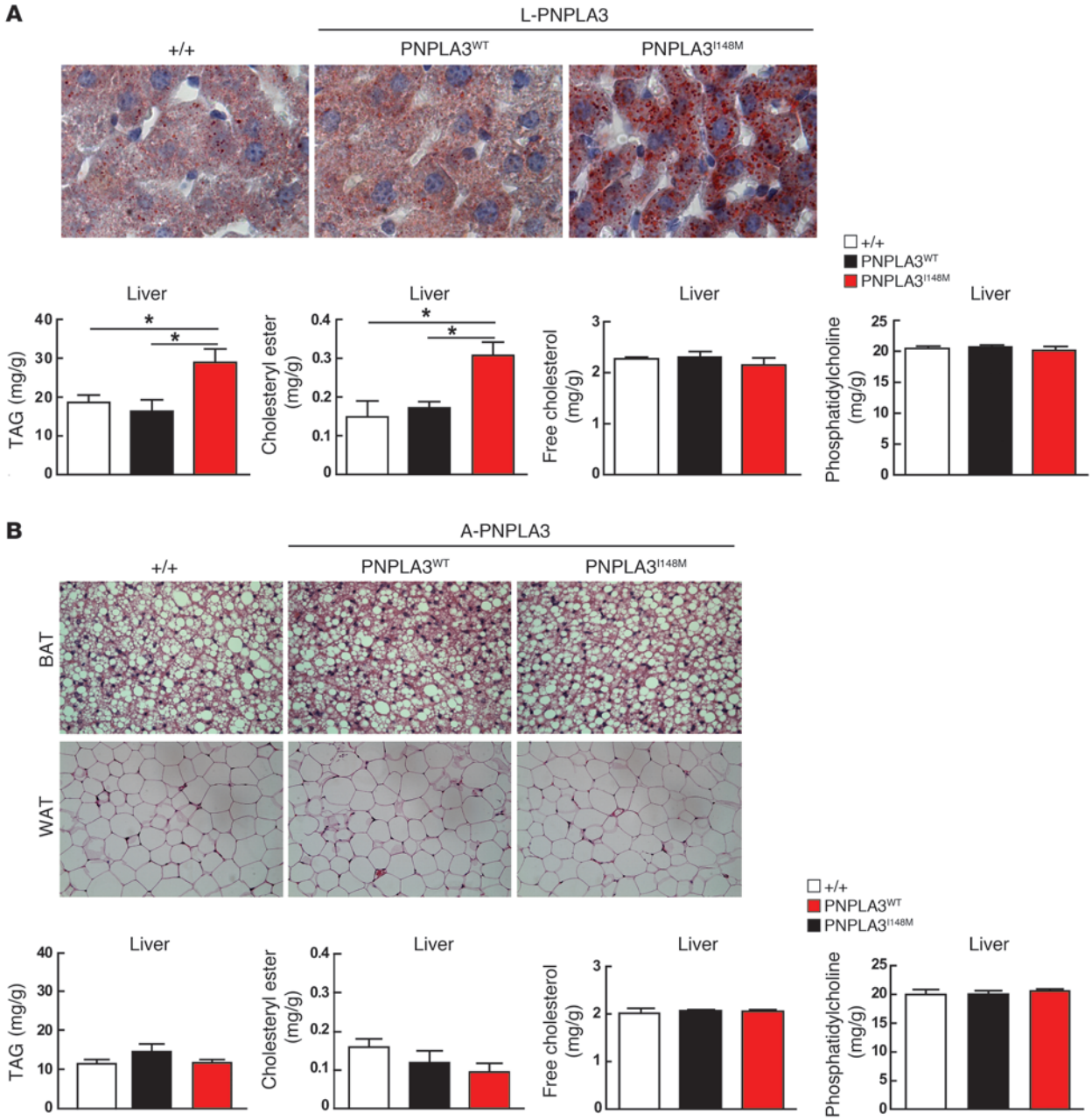

Figure 2

Increased hepatic TAG content in chow-fed PNPLA3^{I148M} transgenic mice. (**A**) Liver sections from 12-week-old chow-fed wild-type (+/+) mice and PNPLA3^{WT} and PNPLA3^{I148M} transgenic male mice (n = 4/group) were stained with Oil Red O and viewed using a Leica microscope (DM2000) (original magnification, ×63). Hepatic lipid levels were measured in the same mice after a 4-hour fast. *P < 0.05. (**B**) Sections from adipose tissue of 12-week-old chow-fed wild-type mice and A-PNPLA3^{WT} and A-PNPLA3^{I148M} mice (n = 4/group) were stained with hematoxylin and eosin (top row). Images of BAT (original magnification, ×40) and WAT (original magnification, ×20) were taken. Hepatic lipid levels were measured after a 4-hour fast. Values are mean ± SEM (n = 4/group). Levels were compared among lines using Student's t tests. The experiment was performed 3 times (n = 4–5 mice/group), and results were similar.

TAG synthesis, ^{3}H-glycerol was injected intraperitoneally into non-transgenic and PNPLA3^{WT} and PNPLA3^{I148M} transgenic mice and the hepatic incorporation into TAG was measured 30 minutes later (Figure 4A and ref. 35). No differences in rates of incorporation of ^{3}H-glycerol into TAG were seen among the 3 lines (Figure 4A). The experiment was repeated using primary hepatocytes from the mice. After 2 hours in culture, cells were incubated in medium containing 0.6 mM oleate plus ^{14}C-glycerol (Figure 4B). Incorporation of label into TAG was monitored for 4 hours, and no significant differences were observed among the lines.

Previous studies have indicated that a majority of the glycerol in hepatic TAG derives from glyceroneogenesis and thus would not

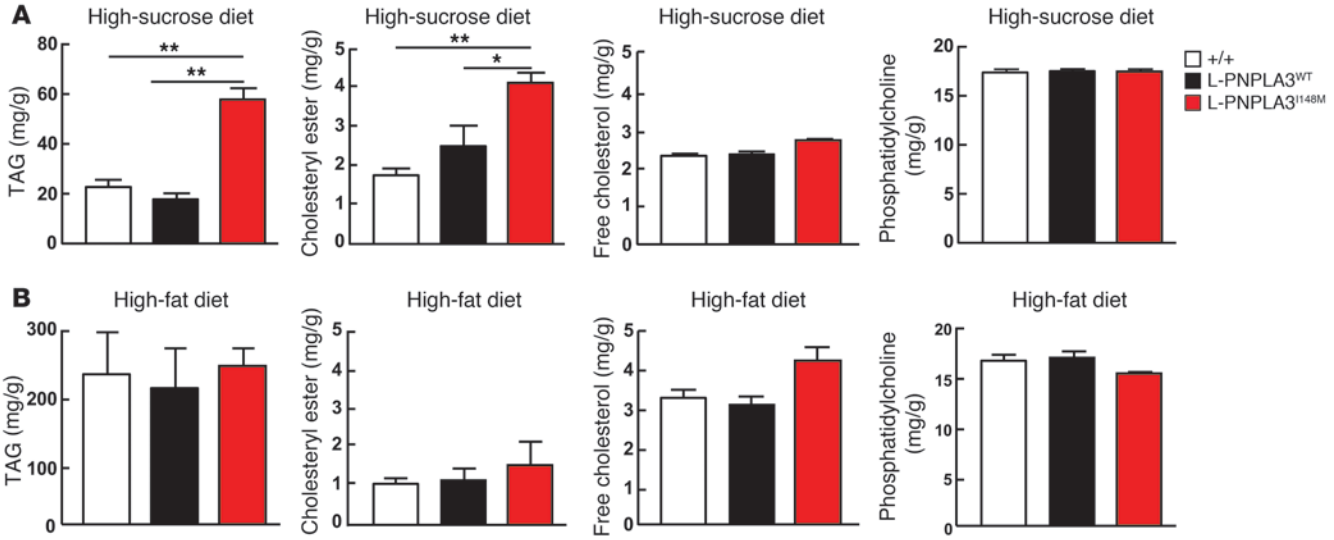

Figure 3

Increased hepatic TAG content in PNPLA3^{I148M} transgenic mice fed a high-sucrose diet. Hepatic lipid levels were measured using enzymatic assays in wild-type mice and PNPLA3^{WT} and PNPLA3^{I148M} transgenic male mice fed (**A**) a high-sucrose (58% sucrose) diet for 6 weeks or (**B**) a high-fat (45% fat) diet for 12 weeks. Mice were killed and livers were collected after a 4-hour fast. Liver lipids were extracted and quantitated using enzymatic assays, as described in Methods. Values are mean ± SEM (n = 5/group). Levels were compared among lines of mice using Student's t test. *P < 0.05,**P < 0.001. The experiment was performed twice (n = 5/group), and results were similar.

be traced by exogenously administered glycerol (36). To avoid artifacts due to the choice of label, the experiments were repeated using ^{14}C-acetate (Figure 4C) and ^{14}C-oleate (Figure 4D). Essentially identical results were obtained with all 3 labels. Since recombinant bacterial PNPLA3 was recently shown to have LPAAT activity in vitro (26), we also compared incorporation of ^{14}C-oleoyl CoA into phosphatidic acid (PA) in hepatic membranes and lipid droplets isolated from the mice: no differences were found among the lines (Figure 4E). Taken together, these data suggest that the increased TAG accumulation in livers of PNPLA3^{I148M} transgenic mice cannot be attributed solely to an increase in hepatic TAG synthesis.

A major pathway for removal of TAG from liver is via secretion as a constituent of VLDLs. To assay the loss of hepatic TAG via this pathway, we inhibited lipolysis of newly secreted VLDL using Triton WR-1339 and measured accumulation of TAG in the blood over time (37). The rate of increase in plasma TAG levels did not differ among the 3 lines (Figure 5A). The experiment was repeated after feeding a high-sucrose diet, and the results were similar (data not shown). Thus, the increase in hepatic TAG in these mice appears not to be caused by defective secretion of VLDL from the liver.

To examine the possibility that PNPLA3^{I148M} impedes TAG hydrolysis, we incubated primary hepatocytes from wild-type and transgenic mice in 0.6 mM oleate plus ^{14}C-glycerol for 4 hours to label cellular TAG. As shown previously, similar amounts of ^{14}C-glycerol were incorporated into TAG among the mouse lines using this protocol (Figure 4B). Triacsin C, an inhibitor of acyl-CoA synthase, was then added to the medium to inhibit incorporation of ^{14}C-acyl-CoA into TAG (38). Cells were washed, and the rate of TAG hydrolysis was determined by monitoring the release of ^{14}C-glycerol into the medium (Figure 5B). In 4 separate experiments, glycerol release was lower in hepatocytes expressing the 148M transgene than the wild-type transgene.

We also measured the rates of fatty acid oxidation in primary hepatocytes from the 3 lines of mice. No differences in O_2 consumption were apparent among the lines, either at baseline or after addition of palmitate. As a positive control for this experiment, we inhibited fatty acid oxidation using etomoxir (39); as expected, a reduction in fatty acid oxidation was seen in the etomoxir-treated cells (Figure 5C).

Effect of PNPLA3^{I148M} on expression of genes involved in hepatic lipid metabolism and inflammation. We measured and compared levels of selected mRNAs that encode proteins involved in transcriptional regulation of hepatic lipids, hepatic fatty acid and TAG synthesis, oxidation, and cholesterol metabolism in the 3 lines of mice (Figure 6). For these experiments, the mice were maintained on a chow diet. Expression of the transgenes did not affect the hepatic mRNA expression levels of mouse *Pnpla3* or of *Atgl*, the patatin family member that is most closely related to PNPLA3. Although no increases in mRNA levels were seen for *SREBP-1c* or *SREBP-2*, several SREBP-1c target genes were significantly increased in the PNPLA3^{I148M} transgenic mice compared with the PNPLA3^{WT} transgenic mice, including *Acc2*, *Fas*, *Scd1*, *Acly*, and *Elovl6*. No increase was found in the mRNA levels of SREBP-2 target genes, including *Hmgcs1* and *Hmgcr*. Levels of mRNAs that are frequently increased in mouse models of hepatic steatosis were also increased in livers of the PNPLA3^{I148M} transgenic mice, including monoacylglycerol O-acyltransferase 1 (*MGAT1*) (40), adipsin (*Cfd*) (41), and cell death–inducing DFFA-like effector C (*Cidec*) (42). The mRNA levels of *Tnfa*, *Col1a1*, and *Acta2*, which are increased in association with hepatic inflammation and fibrosis (43), were not increased in these animals. Similar results were observed in mice fed a high-sucrose diet (data not shown). Interestingly, no increase in SREBP-1c target genes were seen in the transgenic PNPLA3^{I148M} mice fed a high-fat diet; as noted above, a high-fat diet abolishes the differences in liver TAG levels between PNPLA3^{WT} and PNPLA3^{I148M} transgenic mice (Supplemental Figure 6).

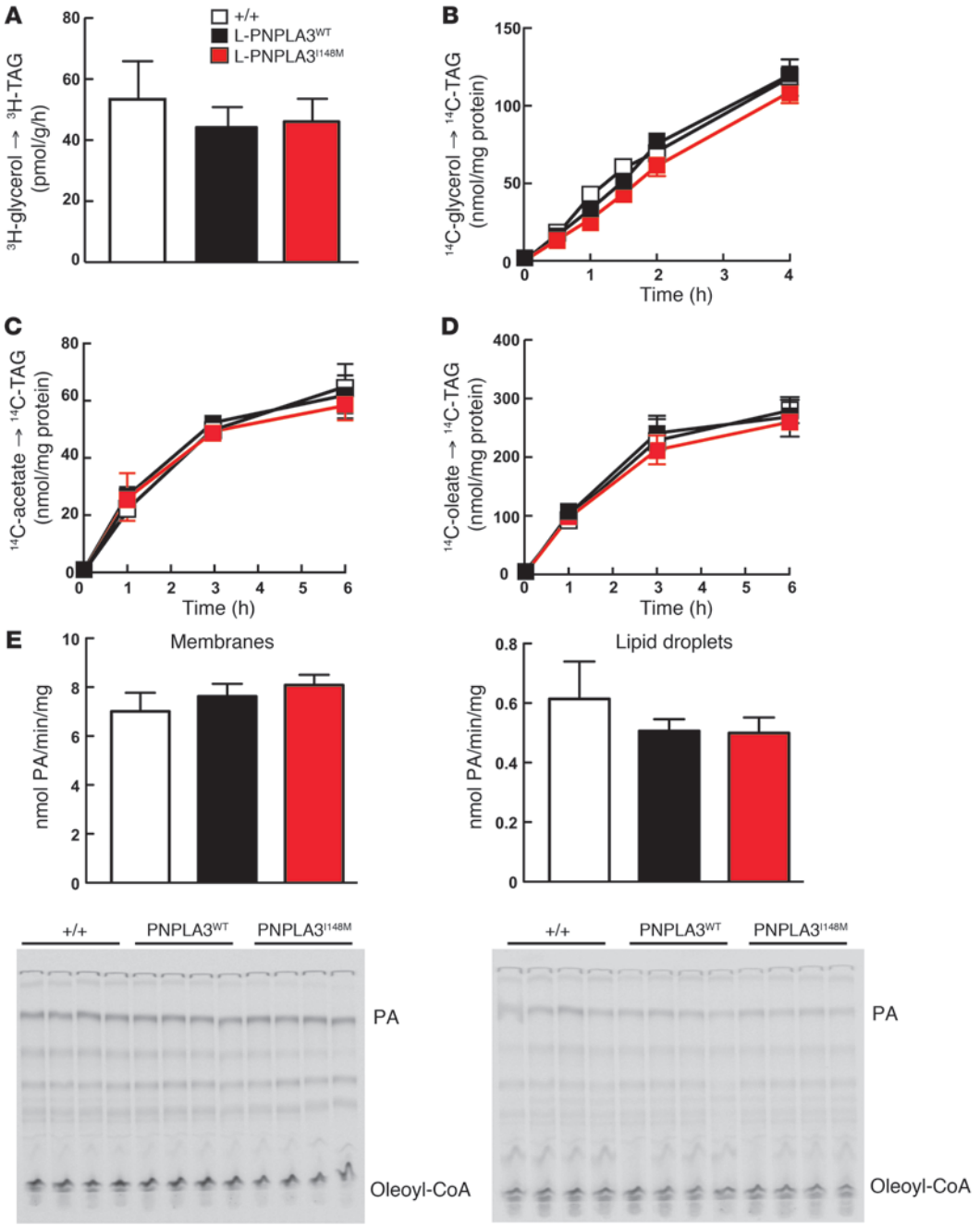

Figure 4

Hepatic lipid synthesis in vivo or in primary hepatocytes from nontransgenic and PNPLA3^{I148M} transgenic mice. (**A**) Incorporation of ^{3}H-glycerol into TAG. Tissue was collected from 8-week-old male mice (n = 4/group) 30 minutes after intraperitoneal injection with ^{3}H-glycerol (1.6 nmol/mouse). (**B**–**D**) Incorporation of metabolic precursors into TAG in primary hepatocytes. Primary hepatocytes from mice of the indicated genotypes were isolated, attached to collagen-coated 6-well plates for 2 hours in triplicate, and then incubated with (**B**) 1.5 mM ^{14}C-glycerol, (**C**) 1.0 mM ^{14}C-acetate, or (**D**) 0.6 mM ^{14}C-oleic acid for the indicated times. Lipids were extracted from the cells, and TAG was isolated by TLC as described in the Methods. (**E**) Measurement of LPAAT activity in membranes and lipid droplets isolated from mice of the indicated genotypes (n = 4/group), as described in the Methods. For the lipid droplet fraction, a total of 2 mg protein was added to 200 ml of buffer (50 mM TrisCl, pH 7.4) plus 200 mM LPA and 5.5 mM ^{14}C-oleoyl-CoA. For the membrane fraction, an additional 50 mM oleoyl-CoA was added to the assay. The experiments were all repeated at least twice, and the results were similar.

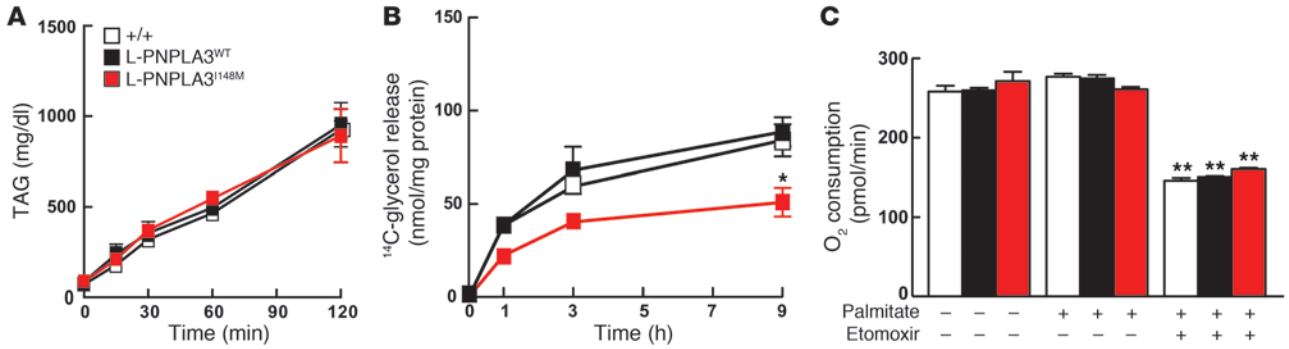

Figure 5

The rate of VLDL-TAG secretion in vivo and TAG hydrolysis and fatty acid oxidation in primary hepatocytes. (**A**) Chow-fed male mice (10–12 weeks old) of the indicated genotypes (n = 5/group) were fasted for 6 hours and injected with Triton WR-1339 (500 mg/kg) to inhibit lipolysis. Blood samples were obtained from the retro-orbital plexus at the times indicated, and plasma TAG levels were measured. Values are mean ± SEM. (**B**) Glycerol release in primary hepatocytes from nontransgenic and transgenic mice. Primary hepatocytes were isolated and plated as described in the legend to Figure 4. Cells were incubated with 1.5 mM ^{14}C-glycerol for 4 hours, washed with ice-cold PBS, and then treated with Triacsin C (5 μM). At the indicated times, medium was removed, and lipids were extracted using the Folch method (58). Radioactivity of ^{14}C-glycerol released from cells into the aqueous phase was quantified. (**C**) Cellular O_2 consumption was measured in primary hepatocytes using the Seahorse XF-24 analyzer. Cells treated with etomoxir (300 mM), an inhibitor of carnitine palmitoyltransferase 1, served as a positive control. Values represent mean ± SEM of triplicate samples. *P < 0.05, **P < 0.01.

Increased incorporation of tritium into fatty acids and TAG in PNPLA3^{I148M} transgenic mice. The increased levels of mRNA encoding several enzymes involved in fatty acid synthesis prompted us to measure hepatic fatty acid synthesis in vivo by monitoring the incorporation of tritium from ^{3}H-H_2O into fatty acids, as previously described (35, 44). For these experiments, the lipids were saponified prior to extraction to release fatty acids. The experiment was performed in chow-fed animals and in animals that were fed a high-sucrose diet for 1 week prior to the injection of label; the results were similar. Fatty acid labeling was increased in the 2 lines of transgenic mice (Figure 7) when compared with that in the control animals. Incorporation was not significantly different between the 2 transgenic lines, although inter-mouse variability may have reduced the power to detect small differences between these groups. We also examined the incorporation of the tritium into PA, DAG, and TAG. No significant differences were observed in PA and DAG. The incorporation into TAG increased progressively from wild-type mice to PNPLA3^{WT} transgenic mice to PNPLA3^{I148M} transgenic mice but reached statistical significance only in the PNPLA3^{I148M} transgenic mice. Thus, we found an increase in TAG synthesis using tritium-labeled water in vivo but not when we used either oleate or glycerol as a label in mice or in cultured hepatocytes. The different results obtained from the experiments using tritiated water in mice and those using glycerol in mice and acetate, oleate, or glycerol in cells may reflect dedifferentiation of the hepatocytes when placed in culture and differences in the biochemical pathways by which the different labels are incorporated (see Discussion).

No differences in phospholipid composition among the 3 lines. The major classes of phospholipids were measured by liquid chromatography (LC) and tandem mass spectrometry (MS) using internal standards (45, 46). No differences were found in the composition of major phospholipid classes in the livers of the 3 lines of mice, even after a high-sucrose diet to maximize the steatosis (Table 1). The PAs, lysophosphatidic acids (LPAs), and DAGs were also measured in an independent laboratory using LC/quadrupole orthogonal time-of-flight (Figure 8A). The LPA levels were lower in the 2 transgenic lines than in the controls, but the differences were not statistically significant. The hepatic PA and DAG levels were similar among the 3 lines.

Relative depletion of long-chain polyunsaturated fatty acids in the TAG of the PNPLA3^{I148M} transgenic mice. To determine the effect of PNPLA3 on hepatic TAG–fatty acid composition, gas chromatography was used to measure and compare the distribution of fatty acids in the hepatic TAG of the 3 lines of mice (Figure 8B). Among the more abundant fatty acids, there were no significant differences in the relative abundance of palmitate (16:0), whereas the ratios of C16:1 and C18:1 fatty acids to total TAG–fatty acids were higher and that of C18:2 fatty acids to total TAG–fatty acids was lower in the PNPLA3^{I148M} transgenic line than in the other 2 lines. Among the less abundant fatty acids, there was a relative depletion of many of the long-chain polyunsaturated fatty acids in the hepatic TAGs of the PNPLA3^{I148M} transgenic mice when compared with those of the PNPLA3^{WT} transgenic or nontransgenic mice. These data indicate that expression of PNPLA3^{I148M} in the liver leads to a relative increase in monounsaturated fatty acids and depletion of long-chain and very-long-chain polyunsaturated fatty acids.

Discussion

The major finding of this study is that transgenic mice overexpressing PNPLA3^{I148M} in the liver recapitulate the fatty liver phenotype as well as other metabolic features associated with this allele in humans. Expression of the 148M allele in mice did not increase body weight or body fat content and was not associated with the adverse metabolic sequelae that often accompany fatty liver, such as insulin resistance or hypertriglyceridemia (2, 47). These results parallel the lack of association between the I148M polymorphism and BMI, insulin resistance, or plasma TAG levels observed in humans (7, 11, 16) and suggest that the metabolic mechanisms by which the 148M allele promotes liver fat accumulation may be similar in mice and humans. Metabolic studies in the transgenic mice revealed that high level expression of PNPLA3^{I148M} in the liver, but not in adipose tissue, affected both hepatic TAG synthe-

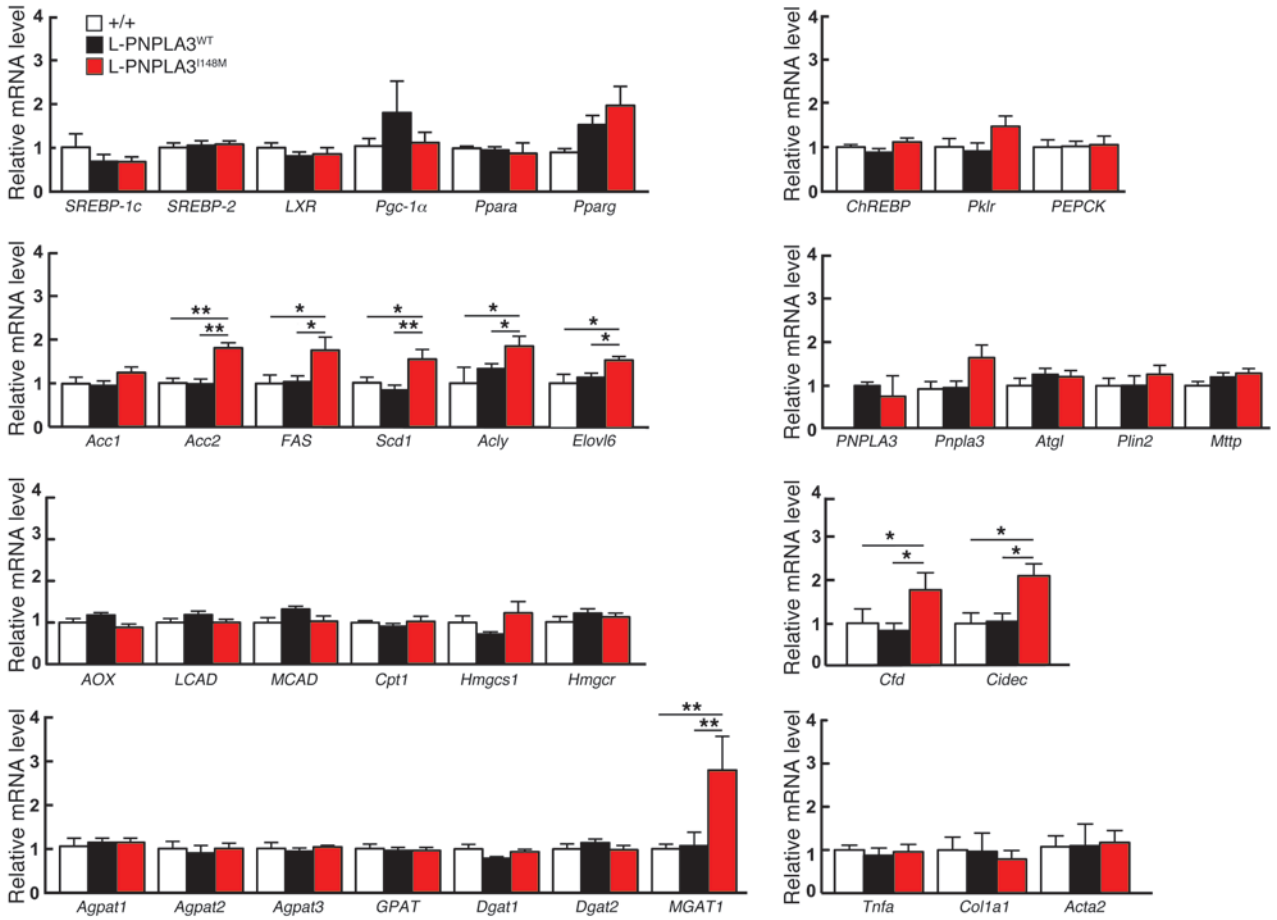

Figure 6

Relative mRNA levels in livers of wild-type and PNPLA3 transgenic mice (n = 4/group). The mice used in this experiment are described in the legend to Figure 2. Total RNA was subjected to real-time PCR quantification, and mRNA levels were expressed relative to levels in nontransgenic mice. Values are mean ± SEM. $^*P < 0.05$, $^{**}P < 0.01$. The experiment was repeated, and the results were similar. *Pgc-1*α, PPARγ co-activator 1α; *ChREBP*, carbohydrate-responsive element–binding protein; *Pklr*, liver pyruvate kinase; *PEPCK*, phosphoenoylpyruvate carboxykinase; *Acc1*, acetyl-CoA carboxylase-1; *Acc2*, acetyl-CoA carboxylase β; *FAS*, fatty acid synthase; *Scd1*, stearoyl-CoA desaturase-1; *Acly*, ATP citrate lyase; *Elovl6*, ELOVL family member 6; *AOX*, acyl-CoA oxidase-1; *LCAD*, long-chain acyl-CoA dehydrogenase; *MCAD*, medium-chain acyl-CoA dehydrogenase; *Cpt1*, carnitine palmitoyltransferase 1; *Hmgcs1*, HMG-CoA synthase; *Hmgcr*, HMG-CoA reductase; *Agpat1*, 1-acylglycerol-3-phosphate O-acyltransferase 1; *Agpat2*, 1-acylglycerol-3-phosphate O-acyltransferase 2; *Agpat3*, 1-acylglycerol-3-phosphate O-acyltransferase 3; *GPAT*, glycerol-3-phosphate acyltransferase; *Dgat1*, diglyceride acyltransferase-1; *Dgat2*, diglyceride acyltransferase-2; *Atgl*, adipose triglyceride lipase; *Mttp*, microsomal TAG transfer protein; *Col1a1*, collagen, type 1α1; *Acta2*, α-smooth muscle actin.

sis and catabolism. A surprising finding was that the PNPLA3^{I148M} transgenic mice have significantly increased fatty acid synthesis and an altered spectrum of TAG–fatty acids in the liver, with no evidence of insulin resistance.

The finding that hepatic TAG levels are normal in mice lacking (24, 25) or overexpressing wild-type PNPLA3 (Figure 2) indicates that the I148M substitution does not cause steatosis by simply increasing or decreasing the normal activity of the enzyme. Metabolic studies performed in vivo and in primary cultured hepatocytes also support a more complex effect of the I148M substitution on hepatic TAG metabolism. Tracer studies provided evidence for increased synthesis and decreased hydrolysis of hepatic TAG in 148M transgenic mice. Changes in the gene expression profile and the fatty acid composition of hepatic TAG in the PNPLA3^{I148M} transgenic mice were consistent with increased de novo fatty acid synthesis in these animals. Taken together, our data indicate that the increased liver fat associated with the I148M substitution is the cumulative result of multiple changes in hepatic TAG metabolism.

Endogenous PNPLA3 is expressed primarily in adipose tissue in mice (27), whereas humans express the gene at highest levels in the liver (28). We failed to observe any consequence of overexpressing wild-type or mutant human PNPLA3 in adipose tissue, despite high levels of transgene expression. No changes were seen in morphology or function of either white or brown fat, and cold tolerance was preserved in the A-PNPLA3^{WT} and A-PNPLA3^{I148M} animals. The increased liver fat content observed in the liver-specific PNPLA3^{I148M} transgenic mice, together with the lack of phenotype in A-PNPLA3^{I148M} mice, is consistent with the notion that the fatty liver phenotype associated with the 148M variant is due to the action of the allele in the liver, rather than adipose tissue.

The finding that PNPLA3^{I148M} causes liver fat accumulation when overexpressed in liver, but not in adipose tissue, is consistent

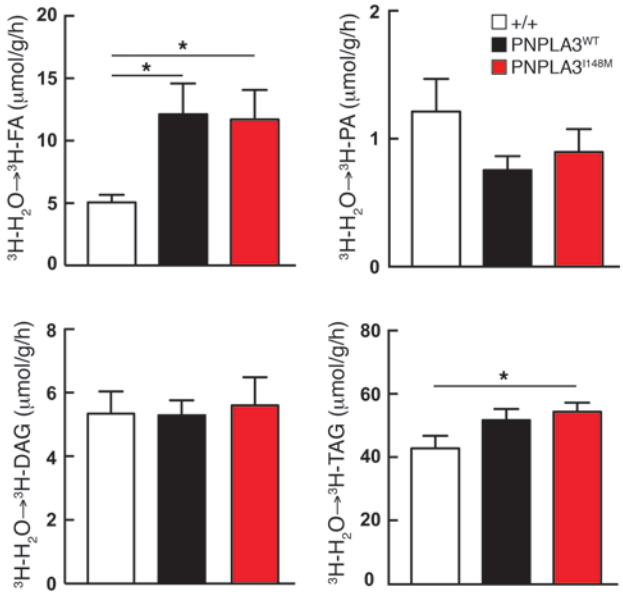

Figure 7
The incorporation of ^{3}H-H$_2$O into fatty acids, PAs, DAGs, and TAGs in livers of 10- to 12-week-old male mice (n = 10/group) fed a high-sucrose diet for 1 week, as described in Methods. Each bar represents mean ± SEM values. FA, fatty acid. *P < 0.01.

with our previous observation that adenovirus-mediated expression of the 148M allele in liver results in increased hepatic fat content (22). The increase in liver TAG levels in the PNPLA3^{I148M} transgenic mice was lower than that observed in mice infected with PNPLA3^{I148M} adenovirus, where hepatic TAG levels increased approximately 5-fold after just 3 days (22). These data indicate that expression of the 148M allele results in a rapid change in hepatic TAG metabolism that quickly stabilizes at a new equilibrium.

Why do PNPLA3^{I148M} transgenic mice develop steatosis on a chow or sucrose diet but not on a high-fat diet? Ingestion of sucrose stimulates de novo synthesis of fatty acids (48), whereas most of the hepatic fatty acids in livers of fat-fed mice are derived from circulating NEFAs. Perhaps PNPLA3 in hepatocytes is exposed preferentially to newly synthesized TAG and is shielded from fatty acids that enter the liver in lipoproteins or are synthesized from circulating NEFAs. Alternatively, PNPLA3 may function specifically under conditions of insulin-stimulated lipid anabolism. The finding that PNPLA3 is virtually absent from livers of fasting animals and is strongly upregulated both transcriptionally (23, 27, 49, 50) and posttranslationally (28) by carbohydrate refeeding is consistent with the latter hypothesis.

It remains possible that the large increase in hepatic TAG levels that occurred in the fat-fed mice (4-fold increase) obscured the differences between the lines. Arguing against this interpretation is the prior observation that hepatic TAG content was increased when the I148M variant was expressed at high levels in the *ob/ob* mice, in which the liver fat levels are appreciably higher than are those of the fat-fed mice in this study (22).

PNPLA3 transgene expression had no detectable effect on 2 of the major pathways used by the liver to remove TAG: VLDL secretion and fatty acid oxidation. TAG hydrolysis (measured as glycerol release) was decreased in hepatocytes from PNPLA3^{I148M} transgenic mice. This decrease in lipolysis in hepatocytes is consistent with the reduction in TAG hydrolysis by the purified recombinant 148M isoform we observed previously in vitro (22). However, liver TAG levels are not increased in *Pnpla3*$^{-/-}$ mice, as would be expected if PNPLA3 was rate limiting for hepatic TAG hydrolysis (24, 25). Thus, the increased liver fat associated with hepatic expression of the 148M allele cannot be due simply to a loss of normal enzyme activity. The 148M allele may have an indirect effect and inhibit lipolysis mediated by other enzymes, such as ATGL, possibly by sequestering a required cofactor or by altering the composition of the lipid droplet.

Nor can the increased hepatic TAG associated with the variant allele be due to an increase in the normal enzyme activity, since we did not observe any increase in hepatic TAG in the mice expressing very high levels of the wild-type enzyme. Kumari et al. (26) reported that a PNPLA3-trigger factor fusion protein catalyzes the acylation of LPA to form PA, a key step in the glycerophosphate pathway for TAG biosynthesis, and that the 148M substitution increases that activity. This gain of function could account for the liver steatosis associated with the 148M allele. We have confirmed that recombinant PNPLA3 has LPAAT activity in vitro when expressed as a fusion protein with trigger factor (data not shown), though we do not observe an increase in LPAAT activity when the recombinant protein is expressed in cultured cells (23). Our data are not compatible with a model in which expression of the PNPLA3^{I148M} variant causes hepatic steatosis simply by increasing hepatic LPAAT activity. We failed to observe a significant, reproducible increase in LPAAT activity in either the membranes or the lipid droplets isolated from the PNPLA3 transgenic mice (Figure 4E). Nor did we

Table 1
Hepatic phospholipid levels in wild-type, L-PNPLA3^{WT}, and L-PNPLA3^{I148M} mice

	WT	PNPLA3^{WT} transgenic	WT	PNPLA3^{I148M} transgenic
PA	2.53 ± 0.18	2.24 ± 0.15	2.89 ± 0.08	2.82 ± 0.08
LPA	0.10 ± 0.01	0.10 ± 0.01	0.11 ± 0.01	0.10 ± 0.01
PC	39.75 ± 0.76	40.37 ± 2.08	38.59 ± 1.15	40.17 ± 1.26
LPC	2.69 ± 0.22	2.60 ± 0.33	3.07 ± 0.18	2.91 ± 0.10
PE	24.68 ± 0.97	26.21 ± 1.56	22.88 ± 1.00	22.47 ± 1.00
LPE	1.40 ± 0.23	1.20 ± 0.12	1.47 ± 0.07	1.22 ± 0.09
PG	8.64 ± 0.53	7.70 ± 0.11	8.99 ± 0.99	9.09 ± 0.66
LPG	0.05 ± 0.00	0.05 ± 0.01	0.04 ± 0.00	0.04 ± 0.00
PI	4.67 ± 0.20	5.06 ± 0.38	4.79 ± 0.25	4.75 ± 0.25
LPI	0.25 ± 0.05	0.11 ± 0.06	0.20 ± 0.02	0.20 ± 0.03
PS	15.08 ± 0.19	14.20 ± 0.32	16.83 ± 0.62	16.11 ± 0.27
LPS	0.15 ± 0.02	0.15 ± 0.05	0.14 ± 0.02	0.12 ± 0.01

Values are mean ± SD of mice (n = 3 per group) fed a high-sucrose diet for 6 weeks. Each line was paired with wild-type littermates. PC, phosphatidylcholine; LPC, lysophosphatidylcholine; PE, phosphatidylethanolamine; LPE, lysophosphatidylethanolamine; PG, phosphatidylglycerol; LPG, lysophosphatidylglycerol; PI, phosphatidylinositol; LPI, lysophosphatidylinositol; PS, phosphatidylserine; LPS, lysophosphatidylserine.

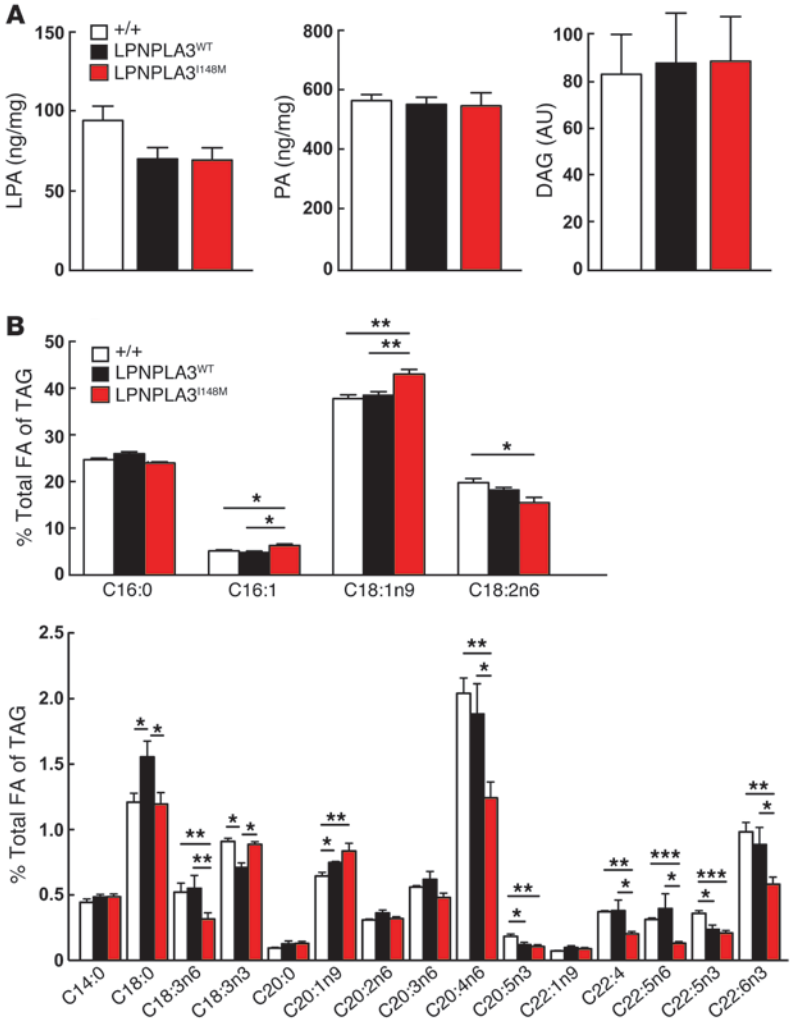

Figure 8
Selected lipid levels and fatty acid composition of TAGs in livers of wild-type and PNPLA3 transgenic mice. (**A**) Levels of LPA, PA, and DAG were measured in the livers of 12- to 13-week-old male wild-type mice and PNPLA3^{WT} and PNPLA3^{I148M} transgenic mice on ad libitum diet (n = 5/group). (**B**) Fatty acid profiles of TAGs in livers of 12- to 13-week-old male mice of the indicated genotypes (n = 5/group). Lipids were extracted from the liver, as described in the Methods, and the TAG fraction was separated by TLC. TAGs were hydrolyzed, and the fatty acids were methyl-esterified and quantified by gas chromatography. Each value represents the mean ± SEM. *P < 0.05, **P < 0.01, ***P < 0.001.

observe an increase in hepatic PA formation in vivo, as determined by tritium incorporation from ^3H-H_2O (Figure 7). Although liver LPA levels were decreased in the transgenic mice (Figure 8A), the decrease was similar in PNPLA3^{WT} transgenic and PNPLA3^{I148M} transgenic animals, yet the PNPLA3^{WT} transgenic animals did not have increased hepatic TAG levels. Liver TAG levels in *Pnpla3*$^{-/-}$ mice are similar to those of WT animals, despite an approximately 50% reduction in LPAAT activity (26). Moreover, overexpression of wild-type PNPLA3 did not increase hepatic TAG concentrations, as would be expected if the enzyme promoted TAG biosynthesis through increased LPAAT activity.

Direct measurements of TAG biosynthesis using glycerol, acetate, and oleate did not reveal differences in the rate of synthesis of hepatic TAG in hepatocytes from the 3 mouse lines. Previous studies have shown that primary hepatocytes from mice lose their responsiveness to insulin/SREBP-1–mediated stimulation of fatty acid and TAG biosynthesis within few hours of being in culture (Jay Horton, personal communication). Since the effect of the transgene is most apparent under conditions in which SREBP-1c is activated (high-sucrose diets), the SREBP pathway may play an important role in 148M-induced steatosis. Accordingly, we examined the 2 major pathways of TAG biosynthesis in intact mice using glycerol and tritiated water as tracers. ^3H-labeled glycerol was incorporated into hepatic TAG at similar rates in all 3 lines. In contrast to these results, incorporation of tritium from ^3H-H_2O into TAG was significantly increased in the PNPLA3^{I148M} transgenic animals, although no differences were found in the incorporation of tritium into PA or DAG. A possible explanation for these seemingly different results is that the 2 tracers label different pathways. Glycerol is converted to glycerophosphate before it is incorporated into LPA, PA, DAG, and ultimately TAG (the glycerophosphate pathway). Tritiated water is incorporated into fatty acids and thus is incorporated into TAG via 2 pathways: the glycerophosphate pathway and by reesterification of monoglycerides with acyl-CoAs (the monoglyceride pathway). The increased incorporation of ^3H-H_2O, but not glycerol, into hepatic TAG in the PNPLA3^{I148M} transgenic mice may reflect increased biosynthesis of hepatic TAG via the monoglyceride pathway. The finding that *MGAT1* mRNA levels were increased in the PNPLA3^{I148M} transgenic mice is consistent with this possibility. Humans with NAFLD have recently been reported to have increased hepatic MGAT activity (51)

Levels of mRNA encoding the lipid droplet–associated protein CIDEC, which were increased in the livers of PNPLA3^{I148M} transgenic mice, are also upregulated in other mouse models of fatty liver disease (52, 53). Expression CIDEC is associated with an increase in the size of cytosolic lipid droplets in various cell types (53). Whether the increased expression of CIDEC contributes to the increased lipid droplet size in this animal model will require additional studies.

Purified recombinant PNPLA3 has been found to have 5 enzymatic activities: TAG, DAG, and MAG hydrolysis (22, 23, 29) as well as acyl-CoA thioesterase (23) and LPAAT activity (26). These different activities are not equally affected by the I148M substitution. In in vitro assays, the I148M substitution results in a substantial loss of TAG, MAG, and DAG hydrolytic activity (23); a modest reduction in acyl-CoA thioesterase activity (23); and an increase in LPAAT activity (26). Considered in isolation, none of these activities alone can explain all of the changes in TAG metabolism observed in the PNPLA3^{I148M} transgenic mice. Therefore, some of the metabolic changes observed in these animals are likely to be secondary rather than direct consequences of altered PNPLA3 activity.

The spectrum of TAG–fatty acids in the livers of both transgenic lines of mice provides further evidence that PNPLA3 expression

affects hepatic TAG composition as well as quantity. The TAG–fatty acid profiles of the PNPLA3^{I148M} transgenic mice (and to a lesser extent the PNPLA3^{WT} transgenic mice) differ significantly from those of wild-type mice and are qualitatively similar to those observed when SREBP-1c is overexpressed in liver (54). The hepatic TAG–fatty acid profile of the PNPLA3^{I148M} transgenic mice is therefore consistent with the increased fatty acid synthesis we observed in these animals (Figure 7). The proportion of long-chain polyunsaturated fatty acids in hepatic TAG was significantly reduced in the transgenic mice (Figure 8B), suggesting that PNPLA3 may play a role in remodeling TAG during the postprandial period. Since long-chain polyunsaturated fatty acids are powerful inhibitors of SREBP-1c (55), expression of the mutant PNPLA3 transgene may lead to increased SREBP-1c activity by lowering polyunsaturated fatty acid levels. The finding that multiple mRNAs of SREBP-1c target genes are increased in the livers of PNPLA3^{I148M} transgenic mice is consistent with this notion.

Simple hepatic steatosis appears to be benign, but a subset of individuals with steatosis develop an inflammatory condition (steatohepatitis) that can progress to cirrhosis (2, 4, 47). The reason why some individuals are more susceptible to the adverse sequelae of increased hepatic TAG levels is not known. The PNPLA3^{I148M} variant has been shown to increase the risk of progressive liver disease, including steatohepatitis and cirrhosis (11). Whether the increased risk of progressive liver disease conferred by the PNPLA3^{I148M} variant results directly from the action of the mutant protein, or is a consequence of the increased risk of steatosis conferred by the allele, is not known. Studies in the PNPLA3^{I148M} transgenic mice may help to address this question and potentially elucidate the factors that mediate the transition from benign steatosis to clinically significant liver disease.

A potential limitation of this model is that the transgene is human and is expressed at higher levels than the endogenous mouse protein. The human and mouse PNPLA3 proteins share 75% sequence identity within the patatin domain but are less similar in the C-terminal half of the proteins. Despite these differences, the wild-type and mutant human proteins appear to traffic normally to the lipid droplet when expressed in the mouse liver (Supplemental Figure 1). We are in the process of developing mice in which the I148M variant has been knocked into the endogenous gene. It remains possible that the fatty liver phenotype requires higher level expression or sequences specific to the human protein.

The relationship between the I148M polymorphism in *PNPLA3* and NAFLD is one of several hundred genetic associations revealed by genome-wide association studies. Whereas these associations can identify genes that contribute to disease processes, in almost all cases the phenotypic effect attributable to the variation is small and the mechanistic basis of the association remains to be defined. The modest phenotypic effects of common sequence variations indicate either that the variation has limited impact on gene function or that the gene is not a major determinant of the phenotype. The finding that neither genetic ablation nor chronic, high level expression of wild-type PNPLA3 affects liver fat content in mice suggests that variation in the normal activity of PNPLA3 is not a major determinant of liver fat content and that the association with fatty liver disease is peculiar to 148M allele. The development of an animal model that recapitulates the metabolic phenotype associated with the allele in humans provides a new in vivo system in which to elucidate the mechanistic relationship between this variant and NAFLD.

Methods

Animals. The human PNPLA3 cDNA was cloned into the *Mlu*I sites of pLiv-11, an expression vector containing a constitutive human apoE gene promoter with a hepatic enhancer (a gift from John Taylor, Gladstone Institute, UCSF, San Francisco, California, USA) (30, 56). After verifying the sequence of the transgene, an 11-kb *Sal*I-*Spe*I fragment containing the promoter elements and the cDNA was isolated and injected into fertilized eggs of C57BL/6J mice to generate transgenic mice as previously described (44). Founder mice were identified by genomic blotting using DNA isolated from their tails (DNeasy Blood and Tissue Kit, Qiagen). Eleven founders for PNPLA3^{WT} transgenic mice and eleven for the PNPLA3^{I148M} transgenic mice were bred to C57BL/6J mice. Mice with the transgene were identified using PCR (primers, 5′-GAGCAAGAATTTGCAACTTGCTACCCATTAG-3′ and 5′-ATGGAGAGGAGGGGGCTGAGAATTGTGTGG-3′) to amplify a 681-bp fragment from human *PNPLA3* and 5′-ATGTATGACCCAGAGCGC CG-3′ plus 5′-GGACAAACCTTCTGCGGCTC-3′ to amplified a 510-bp fragment from mouse *Pnpla3*.

Transgenic mice expressing PNPLA3 predominantly in adipose tissue were developed using an expression construct with an aP2 promoter (31). The human PNPLA3 cDNAs (both wild-type and I148M) were cloned into the S*ma*I sites of pBluescript II SK(+), which contains the 5.4-kb promoter/enhancer of the mouse *Ap2* gene (57). A 7-kb C*la*I-N*ot*I fragment containing the aP2 promoter upstream of PNPLA3 was purified and injected into fertilized eggs to generate transgenic mice (22). Six founders for A-PNPLA3^{WT} and 4 founders for A-PNPLA3^{I148M} mice were identified by genomic blotting and crossed with C57BL/6J mice. Transgenic offspring were identified using PCR and oppositely oriented primers (5′-GCTGGGAGAGATATGCCTTCGAGG-3′ and 5′-GCTGGTGGG-CACTGGAGTGGCAAC-3′) that amplify a 813-bp fragment from the transgene and primers (5′-ATGTATGACCCAGAGCGCCG-3′ and 5′-GGACAAACCTTCTGCGGCTC-3′) that amplify a 510-bp fragment from mouse *Pnpla3*. Mice with the highest level transgenic expression were bred to C57BL/6J for the experiments described in this article.

Lines were established from 3 founder mice for both the L-PNPLA3^{WT} and L-PNPLA3^{I148M} transgenes. Two lines of the A-PNPLA3^{WT} and 3 lines of A-PNPLA3^{I148M} were also established.

All mice were maintained on a 12-hour-light/12-hour-dark cycle and fed the Teklad Mouse/Rat Diet 7001 (Harlan Teklad) ad libitum. The mice used in the experiments were offspring of heterozygous X wild-type matings, and nontransgenic littermates were used as controls.

For the dietary challenge studies, mice were fed a high-fat diet (D12451; 45% kcal from lard, Research Diets) or a high-sucrose diet (no. 901683; MP Biomedicals). Total body fat and lean body mass were determined by nuclear magnetic resonance using the Minispec analyzer (Bruker).

Liver and plasma chemistries. Lipids were extracted from livers (100–200 mg) using the method of Folch and Lees (58). The levels of TAG, cholesterol, cholesteryl ester, free cholesterol, and phosphatidylcholine were measured using enzymatic assays (Infinity, Thermo Electron Corp., and Wako Inc.) and normalized to sample weight. Serum levels of ALT, AST, TAG, cholesterol, and glucose were measured using the Vitros 250 system (GMI Inc.). Enzymatic assay kits were used to determine serum levels of NEFA (Wako Inc.) and ketone bodies (Pointe Scientific Inc.). Serum levels of insulin were measured using an ELISA assay (Crystal Chem Inc.).

Glucose and insulin tolerance testing. Ten-week-old chow-fed mice were fasted for 16 hours prior to intraperitoneal injection of glucose (1.5 g/kg). Plasma levels of glucose were monitored at the indicated times (see Supplemental Figure 2). Insulin tolerance was assessed in mice that were fasted for 4 hours. Human insulin (0.75 unit/kg, Eli Lilly) was injected into the peritoneal fluid, and plasma levels of glucose were measured (Contour, Bayer) prior to the injection and at the indicated time points, as previously described (59).

Tissue morphology. Liver and adipose tissue were collected from isoflurane-anesthetized mice and fixed in 10% formalin for 48 hours and then embedded in paraffin, sectioned, and stained with hematoxylin and eosin. For Oil Red O staining, the liver was fixed in 4% paraformaldehyde for 48 hours and equilibrated in 10% sucrose for 12 hours and then in 18% sucrose for 12 hours at 4°C, prior to cryosectioning by Molecular Pathology Core facility of University of Texas Southwestern Medical Center.

Quantifying the numbers and sizes of lipid droplets. The ImageJ program (NIH) was used to determine the numbers and sizes of lipid droplets in images of Oil Red O–stained sections from the livers of transgenic animals (60). The program classifies the different colors in the images into RGB channel components and calculates the area and pixel value statistics of the image according to user-defined criteria. Oil Red O–stained structures were analyzed in the green channel using the image particle analysis macro as described previously (61).

In vivo lipid metabolism. Incorporation of ^{3}H-glycerol into TAG was measured in 4 chow-fed male mice of each genotype. Mice were injected with ^{3}H-glycerol (1.6 nmol, 133 × 10^{6} dpm/nmol) and killed 30 minutes later. The livers were collected and processed as previously described (35). Incorporation of ^{3}H-H_2O into fatty acids, PA, DAG, and TAG was performed in 2 experiments that included 10 male mice (aged 10–12 weeks). Mice were maintained on a high-sucrose diet for 1 week and then fasted for 1 hour. Mice were then injected with ^{3}H-H_2O (50 mCi in 250 μl 0.9% NaCl) as described previously (35, 44).

To measure VLDL secretion, 5 male mice (aged 10–12 weeks) of each genotype were fasted for 6 hours at the beginning of the light cycle, anesthetized with sodium pentobarbital (80 mg/kg), and then given a bolus of Triton WR-1339 (Tyloxapol; Sigma-Aldrich) (500 mg/kg) via the tail vein (62). Blood was collected from the retro-orbital plexus in EDTA-coated tubes (Microvette 500 KE, Sartedt) at the indicated time points (see Figure 5) and assayed for plasma levels of TAG.

Lipid metabolism in mouse primary hepatocytes. Primary hepatocytes were isolated from the livers of nonfasted wild-type mice and PNPLA3^{WT} and PNPLA3^{I148M} transgenic mice and grown in culture as described previously (63). After 2 hours in culture, cells were washed with PBS. DMEM containing 5% (v/v) delipidated FCS, ^{14}C-glycerol (1 μCi/ml) (American Radiolabeled Chemicals Inc.), 1.5 mM glycerol, 0.6 mM oleic acid, penicillin (100 unit/ml), and streptomycin (100 μg/ml) was added to the cells. Cells were grown at 37°C in 5% CO_2 for the indicated times (see Figure 4). Alternatively, primary hepatocytes were incubated with ^{14}C-acetate (1 μCi/ml) (Perkin Elmer) and 1.0 mM acetate or with ^{14}C-oleic acid (1 μCi/ml), 1.5 mM glycerol, and 0.6 mM oleic acid for the indicated times and then washed 3 times with PBS. Lipids were extracted twice with 1 ml isopropanol/hexane (2:3) for 30 minutes at room temperature and then dried under nitrogen stream (64). Lipids were separated by TLC using hexane/diethyl ether/acetic acid (80:20:1) and visualized with iodine vapor. TAG was scraped from the plate, and the radioactivity was counted using a scintillation counter (Beckman Inc.). Proteins were extracted from delipidated cells by incubating in 1 N NaOH.

To measure TAG hydrolysis, primary hepatocytes were incubated with ^{14}C-glycerol (1 μCi/ml) for 4 hours and then washed twice with ice-cold PBS. Triacsin C (5 μM) in DMEM containing 5% (v/v) delipidated FCS plus penicillin (100 units/ml) and streptomycin (100 ug/ml) was added to the cells. Cells were maintained at 37°C in 5% CO_2 for the indicated time (see Figure 5), and then medium was collected and extracted with 4 ml Folch solution. The aqueous phase was transferred to a scintillation vial, and the radioactivity was quantified.

To measure fatty acid oxidation, primary hepatocytes were seeded at 2 × 10^{4} cells per well on XF-24 cell culture plates (Seahorse Bioscience) coated with rat tail collagen gel in medium containing DMEM with 5% FCS. Cellular oxygen consumption rate was measured as described previously (65). Briefly, after a 4-hour incubation, cells were equilibrated with buffer (111 mM NaCl, 4.7 mM KCl, 2 mM $MgSO_4$, 1.2 mM Na_2HP0_4, 2.5 mM glucose, 0.5 mM carnitine) and incubated at 37°C for 60 minutes prior to addition of palmitate-BSA (200 μm) and etomoxir (300 μm).

RNA expression. Total RNA was isolated from tissues of 4 mice from each group using RNA STAT-60 (Tel-Test Inc.), and Real-Time PCR measurements were performed as previously described (66). Expression levels of PNPLA3^{WT} and PNPLA3^{I148M} hepatic mRNA were measured using oppositely oriented primers (5′-TGCAACTTGCTACCCATTAGGA-3′ and 5′-TCGCAATGGCAGATTCCA-3′). Mouse *36B4* mRNA was used as an internal control.

Tissue fractionation and immunoblotting. Lipid droplets were isolated from the livers of wild-type mice and PNPLA3^{WT} and PNPLA3^{I148M} transgenic mice and from the BAT and WAT of wild-type mice and A-PNPLA3^{WT} and A-PNPLA3^{I148M} mice as described previously (22). Liver, BAT, and WAT tissues (0.2 g) were homogenized in 2 ml of buffer C (20 mM Tris HCl, pH 7.4, 1 mM EDTA) using a Polytron homogenizer and then passed through a 21-gauge needle 25 times. Homogenates were centrifuged (1,000 *g*) for 10 minutes at 4°C and the post-nuclear supernatant (PNS) was adjusted to 20% (w/v) sucrose in buffer C plus 60% sucrose. The PNS was placed at the bottom of a 11.5 ml ultracentrifuge tube (Sorvall) and overlaid with buffer C plus 5% sucrose (5 ml), followed by buffer C alone. The tube was clamped and centrifuged at 28,000 *g* (T-875, Thermo Scientific) for 30 minutes at 4°C. After centrifugation, lipids were isolated, combined with 20 volumes of precooled acetone and stored overnight at –20°C. The precipitated proteins were pelleted by centrifugation at 4,300 *g* for 1 hour at 4°C and then resuspended in buffer C plus 1% SDS. A total of 1% of the lipid droplet protein was size-fractionated on an 8% SDS-PAGE gel, transferred to a nitrocellulose membrane (Amersham Biosciences), and then subjected to immunoblot analysis using a rabbit anti-human PNPLA3 polyclonal antibody directed against the last 20 amino acids of human PNPLA3 (1:1,000 dilution) (22) and a polyclonal antibody to PLIN2 (1:1,000 dilution) (Fitzgerald Industries International). Proteins were visualized using Super-Signal ECL (Pierce Biotechnology).

To measure levels of Akt and phosphorylated Akt, frozen liver was homogenized in modified RIPA buffer (20 mM TrisCl, pH 7.5, 150 mM NaCl, 1 mM EDTA, 1% sodium deoxycholate, 1% NP40, 1 mM sodium orthovanadate, 1 mM PMSF, and 0.1% SDS) with complete protease inhibitors (Roche Diagnostics). A total of 40 μg liver lysate was subjected to immunoblotting as described above using anti-Akt and anti–phospho-Akt (Ser473) mAbs (Cell Signaling).

Core body temperature. Core body temperature was measured as previously described (67). Briefly, mice were fasted for 12 hours and then placed in a cold room (4°C) for 3 hours. Core body temperature was measured using a rectal digital thermometer (Physitemp Instruments Inc.) at the indicated time points (see Supplemental Figure 3).

LPAAT activity of membrane and lipid droplet fractions of mouse liver. Livers were isolated from anesthetized mice and homogenized in 5 ml prechilled lysis buffer (50 mM potassium phosphate, pH 7.0, 0.25 M sucrose, 1 mM DTT, 1 mM EDTA, 20 μg/ml leupeptin, 2 μg/ml antipain, and 1 μg/ml pepstatin). Homogenates were centrifuged for 15 minutes at 9,500 *g* at 4°C. Supernatants were transferred to ultracentrifuge tubes (14 ml) and overlaid with buffer B containing 50 mM potassium phosphate, pH 7.4, 100 mM KCl, 20 μg/ml leupeptin, 2 μg/ml antipain, and 1 μg/ml pepstatin. After centrifugation at 100,000 *g* for 2 hours at 4°C (TH641, Sorvall), lipids were collected and washed with buffer B 3 times. Membranes were washed 3 times with buffer B. To assay LPAAT activity in lipid droplets, 2 μg protein was added to 200 μl of a solution containing 50 mM TrisCl, pH 7.4, 200 μM LPA, and 5.5 μM ^{14}C oleoyl-CoA. To assay enzyme activity in the membrane fraction, additional cold 50 μM oleoyl-CoA was added to the reaction mix. After 10 minutes at 37°C, reactions were transferred to an

ice bath. A total of 1.2 ml of Folch solution was added prior to addition of 2% phosphoric acid (200 μl) to induce phase isolation. The bottom phase was recovered and dried under N_2. The dried lipids were reconstituted in 80 μl chloroform and spotted onto TLC plates. The major classes of lipids were resolved using chloroform/methanol/acetone/acetic acid/water (50:10:20:12:5) as the mobile phase. TLC plates were subjected to phosphorimaging analysis, and bands corresponding to PA were scraped, and the radioactivity was quantified by scintillation counting.

Measurements of selected hepatic lipids in the mice. Lipids were extracted from livers (100–200 mg) and separated into cholesteryl esters, TAGs, and phospholipids using TLC as previously described (68). Fatty acids from the TAG fraction were methyl esterified and separated by gas-LC (GLC) using a Hewlett Packard 6890 Series GC system. The identity of the fatty acid methyl esters was determined by comparing the retention times with fatty acid standards (GLC-744, NU-Chek Prep). The percentage of each fatty acid was calculated in the TAG fraction. Pentadecanoic acid (C15:0) was added as an internal standard. The fatty acid concentration in TAG was calculated based on the area of C15:0 peak.

Phospholipids. Lipid analysis was performed as described in detail elsewhere (45, 46). Briefly, glycerophospholipids from liver tissue were extracted using a modified Bligh and Dyer procedure (69). Frozen mouse liver (~10 mg) was homogenized in 800 μl of ice-cold 0.1 N HCl/CH_3OH (1:1) using a tight-fit glass homogenizer (Kimble/Kontes Glass Co.) for about 1 minute on ice. The suspension was then transferred to cold 1.5 ml Eppendorf tubes and vortexed with 400 μl of cold $CHCl_3$ for 1 minute. The extraction proceeded with centrifugation (5 minutes, 4°C, 18,000 *g*) to separate the 2 phases. The lower organic layer was collected and solvent evaporated. The resulting lipid film was dissolved in 100 μl of mobile phase A [isopropanol/hexane/100 mM NH_4COOH (aq) (58:40:2)]. Quantification of glycerophospholipids was achieved by the use of an LC/MS technique, employing synthetic odd-carbon diacyl and lysophospholipid standards. Typically, 200 ng of each odd-carbon standard was added per 10 to 20 mg tissue. Glycerophospholipids were analyzed on an Applied Biosystems/MDS SCIEX 4000 Q TRAP hybrid triple quadrupole/linear ion trap mass spectrometer (Applied Biosystems) and a Shimadzu high-pressure LC system with a Phenomenex Luna Silica column (2 × 250 mm, 5-μm particle size) using a gradient elution as previously described (39, 40). The identification of the individual species, achieved by LC/MS/MS, was based on their chromatographic and mass spectral characteristics. This analysis allows identification of the 2 fatty acid moieties but does not differentiate relative position on the glycerol backbone (*sn-1* versus *sn-2*).

LPA, PA, and DAG analysis by high-resolution LC/MS. To measure hepatic levels of LPA and PA in the transgenic mice, 400 μl PBS was added to 50 mg liver tissue, and the mixture was spiked with 5 μg/ml LPA 17:0 (Avanti Polar Lipids Inc.). Samples were homogenized using a Precellys 24 homogenizer (Bertin Technologies) (5,500 rpm, twice for 30 seconds, with a 15-second pause). Citrate buffer (400 μl, pH 4.0) was added to the sample, and the mixture was centrifuged (42,500 *g*, 10 minutes) at 5°C. Lipids were extracted using acidic butanol (1 ml) followed by saturated butanol (0.5 ml) as described previously (70). The extracted fractions were combined and evaporated under N_2 at room temperature, and the dried extract was reconstituted in 50% water, 50% methanol, 0.1% dimethylisopropylamine (DMIPA), and 5% acetic acid (100 μl). A total of 20 μl of the extract was injected into a LC (UPLC, Waters Corp) coupled to a MS QTOF (Synapt G2 HDMS, Waters Corp). Separation was performed using an Acquity Symmetry 300Å C4 (2.1 × 100 mm) column with a particle size of 1.7 μm (Waters Corp) that was maintained at 90°C. External calibration curves were constructed using standards ranging from 0.001 to 2 μg/ml (Avanti Polar Lipids Inc.) to measure the following species of LPA (16:0, 16:1, 18:0, 18:1, 18:2, 20:4, 22:6) and PA (16:0/18:1, 16:0/18:2, 16:0/20:4, 18:0/20:4). Flow rate was set at 0.3 ml/min. A gradient started at 90% mobile phase A (H_2O plus 0.2% DMIPA) and 10% mobile phase B (isopropanol plus methanol [90/10, v/v] with 0.2 % DMIPA) was ramped to 77% mobile phase A over 4 minutes and then reduced progressively to 30% over 10 minutes and was at 1% within 11.5 minutes. The gradient was held for 1 minute at 1% mobile phase A and then equilibrated to the starting conditions for 3 minutes. The MS was operated in negative ion ionization mode at 20,000 full-width half-mass resolution (FWHM), and acquisition ranged from 100 to 1,000 m/z.

Neutral lipids were extracted from liver tissue (50 mg) after adding 20 μl of an internal standard solution containing 2 μg/ml TAG 51:0 (Avanti Polar Lipids Inc.). Dichloromethane/methanol (2:1) (1 ml) was added, and the samples were homogenized (42,500 *g*, twice for 30 seconds, with a 15-second pause) (69). Water (200 μl) was added, and the sample was vortexed for 30 seconds before the homogenate was centrifuged at 42,500 *g* at 5°C for 10 minutes. A total of 10 μl of the lower layer (organic phase) was transferred to an LC vial and diluted in 490 μl of injection solvent (65% acetonitrile, 30% isopropanol, 5% water) and analyzed by LC/MS exactly as described previously (71). Data was normalized for liver weights. Since the measurement of DAGs was used in an untargeted profile mode and standards were not available, the data are reported as AUC. The internal standard was used to calculate a response ratio (analyte/internal standard) and the data were scaled using Pareto scaling, which uses the square root of SD as the scaling factor.

Statistics. All data are presented as mean ± SEM. Differences among group means were assessed by a 2-tailed, nonpaired Student's *t* test using the Graphpad Prism statistical software (Graphpad Software Inc.). Results were considered statistically significant at $P < 0.05$.

Study approval. All animal experiments were performed with the approval of the Institutional Animal Care and Research Advisory Committee at University of Texas Southwestern Medical Center at Dallas.

Acknowledgments

We wish to thank Christina Zhao, Fang Xu, Stephanie Blankenship, and Norma Anderson for excellent technical assistance. We also thank Robert Hammer for the development of the transgenic mice in the UT Southwestern Transgenic Core Facility. We thank Jay Horton, Young-Ah Moon, Shawn Burgess, Elizabeth Parks, John Shelton, and Guosheng Liang for helpful discussions. Steve Milne and David Myers contributed to the mass spectrometry–based lipid identification and analysis. This work was supported by grants from the NIH (HL20948, 1HL092550, DK090066, and GM 069338).

Received for publication June 5, 2012, and accepted in revised form August 9, 2012.

Address correspondence to: Helen H. Hobbs or Jonathan C. Cohen, Department of Molecular Genetics, University of Texas Southwestern Medical Center, 5323 Harry Hines Boulevard, Dallas, Texas 75390-9046, USA. Phone: 214.648.6724; Fax: 214.648.7539; E-mail: Helen.hobbs@utsouthwestern.edu (H.H. Hobbs), jonathan.cohen@utsouthwestern.edu (J.C. Cohen).

1. Ludwig J, Viggiano TR, McGill DB, Oh BJ. Nonalcoholic steatohepatitis: Mayo Clinic experiences with a hitherto unnamed disease. *Mayo Clin Proc*. 1980;55(7):434–438.
2. Day CP, James OF. Steatohepatitis: a tale of two "hits"? *Gastroenterology*. 1998;114(4):842–845.
3. Browning JD, et al. Prevalence of hepatic steatosis in an urban population in the United States: impact of ethnicity. *Hepatology*. 2004;40(6):1387–1395.
4. Cohen JC, Horton JD, Hobbs HH. Human fatty liver disease: old questions and new insights. *Science*. 2011;332(6037):1519–1523.
5. Speliotes EK, et al. Genome-wide association analysis identifies variants associated with nonalcoholic fatty liver disease that have distinct effects on meta-

bolic traits. *PLoS Genet*. 2011;7(3):e1001324.
6. Baulande S, Lassnier F, Lucas M, Pairault J. Adiponutrin, a transmembrane protein corresponding to a novel dietary - and obesity-linked mRNA specifically expressed in the adipose lineage. *J Biol Chem*. 2001;276(36):33336–33344.
7. Romeo S, et al. Genetic variation in PNPLA3 confers susceptibility to nonalcoholic fatty liver disease. *Nat Genet*. 2008;40(12):1461–1465.
8. Sookoian S, Castano GO, Burgueno AL, Gianotti TF, Rosselli MS, Pirola CJ. A nonsynonymous gene variant in the adiponutrin gene is associated with nonalcoholic fatty liver disease severity. *J Lipid Res*. 2009;50(10):2111–2116.
9. Hotta K, et al. Association of the rs738409 polymorphism in PNPLA3 with liver damage and the development of nonalcoholic fatty liver disease. *BMC Med Genet*. 2010;11(1):172.
10. Rotman Y, Koh C, Zmuda JM, Kleiner DE, Liang TJ. The association of genetic variability in patatin-like phospholipase domain-containing protein 3 (PNPLA3) with histological severity of nonalcoholic fatty liver disease. *Hepatology*. 2010;52(3):814–903.
11. Sookoian S, Pirola CJ. Meta-analysis of the influence of I148M variant of patatin-like phospholipase domain containing 3 gene (PNPLA3) on the susceptibility and histological severity of nonalcoholic fatty liver disease. *Hepatology*. 2011;53(6):1883–18894.
12. Falleti E, et al. PNPLA3 rs738409C/G polymorphism in cirrhosis: relationship with the aetiology of liver disease and hepatocellular carcinoma occurrence. *Liver Int*. 2011;31(8):1137–1143.
13. Valenti L, et al. Patatin-like phospholipase domain-containing 3 I148M polymorphism, steatosis, and liver damage in chronic hepatitis C. *Hepatology*. 2011;53(3):791–799.
14. Trepo E, et al. Common polymorphism in the PNPLA3/adiponutrin gene confers higher risk of cirrhosis and liver damage in alcoholic liver disease. *J Hepatol*. 2011;55(4):906–912.
15. Valenti L, et al. Homozygosity for the patatin-like phospholipase-3/adiponutrin I148M polymorphism influences liver fibrosis in patients with nonalcoholic fatty liver disease. *Hepatology*. 2010;51(4):1209–1217.
16. Speliotes EK, Butler JL, Palmer CD, Voight BF, Hirschhorn JN. PNPLA3 variants specifically confer increased risk for histologic nonalcoholic fatty liver disease but not metabolic disease. *Hepatology*. 2010; 52(3):904–912.
17. Burza MA, et al. PNPLA3 I148M (rs738409) genetic variant is associated with hepatocellular carcinoma in obese individuals [published online ahead of print June 13, 2012]. *Dig Liver Dis*. doi:10.1016/j.dld.2012.05.006.
18. Tian C, Stokowski RP, Kershenobich D, Ballinger DG, Hinds DA. Variant in PNPLA3 is associated with alcoholic liver disease. *Nat Genet*. 2010;42(1):21–23.
19. Stickel F, et al. Genetic variation in the PNPLA3 gene is associated with alcoholic liver injury in caucasians. *Hepatology*. 2011;53(1):86–95.
20. Racusen D, Foote M. A major soluble glycoprotein of potato tubers. *J Food Biochem*. 1980;4:43–52.
21. Rydel TJ, et al. The crystal structure, mutagenesis, and activity studies reveal that patatin is a lipid acyl hydrolase with a ser-asp catalytic dyad. *Biochem*. 2003;42(22):6696–6708.
22. He S, et al. A sequence variation (I148M) in PNPLA3 associated with nonalcoholic fatty liver disease disrupts triglyceride hydrolysis. *J Biol Chem*. 2010; 285(9):6706–6715.
23. Huang Y, Cohen JC, Hobbs HH. Expression and characterization of a PNPLA3 protein isoform (I148M) associated with nonalcoholic fatty liver disease. *J Biol Chem*. 2011;286(43):37085–37093.
24. Basantani MK, et al. Pnpla3/Adiponutrin deficiency in mice does not contribute to fatty liver disease or metabolic syndrome. *J Lipid Res*. 2011;52(2):318–329.
25. Chen W, Chang B, Li L, Chan L. Patatin-like phospholipase domain-containing 3/adiponutrin deficiency in mice is not associated with fatty liver disease. *Hepatology*. 2010;52(3):1134–1142.
26. Kumari M, et al. Adiponutrin functions as a nutritionally regulated lysophosphatidic acid acyltransferase. *Cell Metab*. 2012;15(5):691–702.
27. Lake AC, et al. Expression, regulation, and triglyceride hydrolase activity of adiponutrin family members. *J Lipid Res*. 2005;46(11):2477–2487.
28. Huang Y, et al. A feed-forward loop amplifies nutritional regulation of PNPLA3. *Proc Natl Acad Sci U S A*. 2010;107(17):7892–7897.
29. Jenkins CM, Mancuso DJ, Yan W, Sims HF, Gibson B, Gross RW. Identification, cloning, expression, and purification of three novel human calcium-independent phospholipase A_2 family members possessing triacylglycerol lipase and acylglycerol transacylase activities. *J Biol Chem*. 2004;279(47):48968–48975.
30. Simonet WS, Bucay N, Lauer SJ, Taylor JM. A far-downstream hepatocyte-specific control region directs expression of the linked human apolipoprotein E and C-I genes in transgenic mice. *J Biol Chem*. 1993;268(11):8221–8229.
31. Hunt CR, Ro JH, Dobson DE, Min HY, Spiegelman BM. Adipocyte P2 gene: developmental expression and homology of 5′-flanking sequences among fat cell-specific genes. *Proc Natl Acad Sci U S A*. 1986; 83(11):3786–3790.
32. Olsson M, et al. Establishment of a transgenic mouse model specifically expressing human serum amyloid A in adipose tissue. *PLoS One*. 2011;6(5):e19609.
33. Seale P, et al. Prdm16 determines the thermogenic program of subcutaneous white adipose tissue in mice. *J Clin Invest*. 2011;121(1):96–105.
34. Oliver P, Caimari A, Diaz-Rua R, Palou A. Cold exposure down-regulates adiponutrin/PNPLA3 mRNA expression and affects its nutritional regulation in adipose tissues of lean and obese Zucker rats. *Br J Nutr*. 2012;107(9):1–13.
35. Guan HP, Goldstein JL, Brown MS, Liang G. Accelerated fatty acid oxidation in muscle averts fasting-induced hepatic steatosis in SJL/J mice. *J Biol Chem*. 2009;284(36):24644–24652.
36. Nye CK, Hanson RW, Kalhan SC. Glyceroneogenesis is the dominant pathway for triglyceride glycerol synthesis in vivo in the rat. *J Biol Chem*. 2008;283(41):27565–27574.
37. Millar JS, Cromley DA, McCoy MG, Rader DJ, Billheimer JT. Determining hepatic triglyceride production in mice: comparison of poloxamer 407 with Triton WR-1339. *J Lipid Res*. 2005;46(9):2023–2028.
38. Igal RA, Wang P, Coleman RA. Triacsin C blocks de novo synthesis of glycerolipids and cholesterol esters but not recycling of fatty acid into phospholipid: evidence for functionally separate pools of acyl-CoA. *Biochem J*. 1997;324(Pt 2):529–534.
39. Reaven GM, Chang H, Hoffman BB. Additive hypoglycemic effects of drugs that modify free-fatty acid metabolism by different mechanisms in rats with streptozocin-induced diabetes. *Diabetes*. 1988; 37(1):28–32.
40. Yen CL, Stone SJ, Cases S, Zhou P, Farese RV Jr. Identification of a gene encoding MGAT1, a monoacylglycerol acyltransferase. *Proc Natl Acad Sci U S A*. 2002;99(13):8512–8517.
41. Min HY, Spiegelman BM. Adipsin, the adipocyte serine protease: gene structure and control of expression by tumor necrosis factor. *Nucleic Acids Res*. 1986;14(22):8879–8892.
42. Danesch U, Hoeck W, Ringold GM. Cloning and transcriptional regulation of a novel adipocyte-specific gene, FSP27. CAAT-enhancer-binding protein (C/EBP) and C/EBP-like proteins interact with sequences required for differentiation-dependent expression. *J Biol Chem*. 1992; 267(10):7185–7193.
43. Hernandez-Gea V, Friedman SL. Pathogenesis of liver fibrosis. *Annu Rev Pathol*. 2011;6:425–456.
44. Shimano H, Horton JD, Hammer RE, Shimomura I, Brown MS, Goldstein JL. Overproduction of cholesterol and fatty acids causes massive liver enlargement in transgenic mice expressing truncated SREBP-1a. *J Clin Invest*. 1996;98(7):1575–1584.
45. Myers DS, Ivanova PT, Milne SB, Brown HA. Quantitative analysis of glycerophospholipids by LC-MS: acquisition, data handling, and interpretation. *Biochim Biophys Acta*. 2011;1811(11):748–757.
46. Ivanova PT, Milne SB, Byrne MO, Xiang Y, Brown HA. Glycerophospholipid identification and quantitation by electrospray ionization mass spectrometry. *Methods Enzymol*. 2007;432:21–57.
47. Neuschwander-Tetri BA, Caldwell SH. Nonalcoholic steatohepatitis: summary of an AASLD Single Topic Conference. *Hepatology*. 2003; 37(5):1202–1219.
48. Cohen AM, Teitelbaum A. Effect of glucose, fructose, sucrose and starch on lipgenesis in rats. *Life Sci*. 1968;7(2):23–29.
49. Polson DA, Thompson MP. Adiponutrin mRNA expression in white adipose tissue is rapidly induced by meal-feeding a high-sucrose diet. *Biochem Biophy Res Comm*. 2003;301(2):261–266.
50. Kershaw EE, Hamm JK, Verhagen LA, Peroni O, Katic M, Flier JS. Adipose triglyceride lipase: function, regulation by insulin, and comparison with adiponutrin. *Diabetes*. 2006;55(1):148–157.
51. Hall AM, et al. Evidence for regulated monoacylglycerol acyltransferase expression and activity in human liver. *J Lipid Res*. 2012;53(5):990–999.
52. Matsusue K, et al. Hepatic steatosis in leptin-deficient mice is promoted by the PPARgamma target gene Fsp27. *Cell Metab*. 2008;7(4):302–311.
53. Gong J, et al. Fsp27 promotes lipid droplet growth by lipid exchange and transfer at lipid droplet contact sites. *J Cell Biol*. 2011;195(6):953–963.
54. Shimomura I, Shimano H, Korn BS, Bashmakov Y, Horton JD. Nuclear sterol regulatory element-binding proteins activate genes responsible for the entire program of unsaturated fatty acid biosynthesis in transgenic mouse liver. *J Biol Chem*. 1998; 273(52):35299–35306.
55. Ou J, et al. Unsaturated fatty acids inhibit transcription of the sterol regulatory element-binding protein-1c (SREBP-1c) gene by antagonizing ligand-dependent activation of the LXR. *Proc Natl Acad Sci U S A*. 2001;98(11):6027–6032.
56. Allan CM, Taylor JM. Expression of a novel human apolipoprotein (apoC-IV) causes hypertriglyceridemia in transgenic mice. *J Lipid Res*. 1996; 37(7):1510–1518.
57. Ross SR, et al. A fat-specific enhancer is the primary determinant of gene expression for adipocyte P2 in vivo. *Proc Natl Acad Sci U S A*. 1990;87(24):9590–9594.
58. Folch J, Lees M, Sloane Stanley GH. A simple method for the isolation and purification of total lipides from animal tissues. *J Biol Chem*. 1957;226(1):497–509.
59. Li JZ, et al. Cideb regulates diet-induced obesity, liver steatosis, and insulin sensitivity by controlling lipogenesis and fatty acid oxidation. *Diabetes*. 2007;56(10):2523–2532.
60. Singh R, et al. Autophagy regulates lipid metabolism. *Nature*. 2009;458(7242):1131–1135.
61. Ramirez-Zacarias JL, Castro-Munozledo F, Kuri-Harcuch W. Quantitation of adipose conversion and triglycerides by staining intracytoplasmic lipids with Oil red O. *Histochemistry*. 1992;97(6):493–497.
62. Jones C, et al. Disruption of LDL but not VLDL clearance in autosomal recessive hypercholesterolemia. *J Clin Invest*. 2007;117(1):165–174.
63. Matsuda M, et al. SREBP cleavage-activating protein (SCAP) is required for increased lipid synthesis in liver induced by cholesterol deprivation and insulin elevation. *Genes Dev*. 2001;15(10):1206–1216.
64. Cortes VA, et al. Molecular mechanisms of hepatic steatosis and insulin resistance in the AGPAT2-deficient mouse model of congenital generalized lipodystrophy. *Cell Metab*. 2009;9(2):165–176.
65. Nasrin N, et al. SIRT4 regulates fatty acid oxida-

tion and mitochondrial gene expression in liver and muscle cells. *J Biol Chem*. 2010;285(42):31995–32002.
66. Engelking LJ, et al. Overexpression of Insig-1 in the livers of transgenic mice inhibits SREBP processing and reduces insulin-stimulated lipogenesis. *J Clin Invest*. 2004;113(8):1168–1175.
67. Zhou Z, et al. Cidea-deficient mice have lean phenotype and are resistant to obesity. *Nat Genet*. 2003; 35(1):49–56.
68. Moon YA, Hammer RE, Horton JD. Deletion of ELOVL5 leads to fatty liver through activation of SREBP-1c in mice. *J Lipid Res*. 2009;50(3):412–423.
69. Bligh EG, Dyer WJ. A rapid method of total lipid extraction and purification. *Can J Biochem Physiol*. 1959;37(8):911–917.
70. Scherer M, Schmitz G, Liebisch G. High-throughput analysis of sphingosine 1-phosphate, sphinganine 1-phosphate, and lysophosphatidic acid in plasma samples by liquid chromatography-tandem mass spectrometry. *Clin Chem*. 2009;55(6):1218–1222.
71. Castro-Perez J, et al. Anacetrapib promotes reverse cholesterol transport and bulk cholesterol excretion in Syrian golden hamsters. *J Lipid Res*. 2011; 52(11):1965–1973.